Biophysical Journal
Article

Biophysical Society

$GABA_A$ receptor subunit M2-M3 linkers have asymmetric roles in pore gating and diazepam modulation

Joseph W. Nors,[1,2] Zachary Endres,[1] and Marcel P. Goldschen-Ohm[1,*]
[1]Department of Neuroscience, University of Texas at Austin, Austin, Texas and [2]Department of Molecular and Cellular Physiology, Stanford University, Stanford, California

ABSTRACT $GABA_A$ receptors ($GABA_A$Rs) are neurotransmitter-gated ion channels critical for inhibitory synaptic transmission as well as the molecular target for benzodiazepines (BZDs), one of the most widely prescribed class of psychotropic drugs today. Despite structural insight into the conformations underlying functional channel states, the detailed molecular interactions involved in conformational transitions and the physical basis for their modulation by BZDs are not fully understood. We previously identified that alanine substitution at the central residue in the α1 subunit M2-M3 linker (V279A) enhances the efficiency of linkage between the BZD site and the pore gate. Here, we expand on this work by investigating the effect of alanine substitutions at the analogous positions in the M2-M3 linkers of β2 (I275A) and γ2 (V290A) subunits, which together with α1 comprise typical heteromeric $\alpha1\beta2\gamma2$ synaptic $GABA_A$Rs. We find that these mutations confer subunit-specific effects on the intrinsic pore closed-open equilibrium and its modulation by the BZD diazepam (DZ). The mutations α1(V279A) or γ2(V290A) bias the channel toward a closed conformation, whereas β2(I275A) biases the channel toward an open conformation to the extent that the channel becomes leaky and opens spontaneously in the absence of agonist. In contrast, only α1(V279A) enhances the efficiency of DZ-to-pore linkage, whereas mutations in the other two subunits have no effect. These observations show that the central residue in the M2-M3 linkers of distinct subunits in synaptic $\alpha1\beta2\gamma2$ $GABA_A$Rs contribute asymmetrically to the intrinsic closed-open equilibrium and its modulation by DZ.

SIGNIFICANCE $GABA_A$ receptors are pentameric ligand-gated ion channels that regulate inhibitory signaling throughout the central nervous system. Although many subtypes are comprised of combinations of several different subunits, structural and functional observations have begun to paint a general picture of largely pseudo-symmetric conformational changes in each subunit. Here, we show that the flexibility of an important gating loop has subunit-specific asymmetric effects on the energetics of channel activation and drug modulation. This work illustrates that different subunits can apply non-symmetric and even opposing forces on the gating conformational change.

INTRODUCTION

$GABA_A$Rs are the primary neurotransmitter-gated ion channels mediating inhibitory synaptic signaling throughout the central nervous system (1). They belong to the superfamily of cys-loop pentameric ligand-gated ion channels (pLGICs) including glycine, nicotinic acetylcholine, and serotonin receptors (2). Genetic mutations conferring $GABA_A$R dysfunction are associated with human disorders including epilepsy, autism spectrum disorder, intellectual disability, schizophrenia, and neurodevelopment disorders such as fragile X syndrome (3–9). $GABA_A$Rs are also the molecular target for numerous anxiolytic, analgesic, and sedative compounds. One of the most widely prescribed classes of psychotropic drugs are benzodiazepines (BZDs) (10), whose modulation of $GABA_A$R activity is used to treat neurological conditions including anxiety, insomnia, muscle spasms, pain, and epilepsy (11). Many functional studies together with recent cryogenic electron microscopy (cryo-EM) structural models of heteromeric synaptic $GABA_A$Rs have begun to paint a picture of the conformational landscape involved in channel gating. However, a comprehensive view of the molecular details that govern the energetics of conformational transitions remains incomplete. Furthermore, the mechanism for allosteric modulation by drugs such as BZDs are only poorly understood (12).

Submitted October 30, 2023, and accepted for publication February 20, 2024.

*Correspondence: marcel.goldschen-ohm@austin.utexas.edu
Joseph W. Nors and Zachary Endres contributed equally to this work.

Editor: Brad Rothberg.
https://doi.org/10.1016/j.bpj.2024.02.016

Typical synaptic $GABA_ARs$ are heteropentamers comprised of α1, β1-3, and γ2 subunits (Fig. 1) (13,14). The M2-M3 linker at the interface between the extracellular domain (ECD) and the transmembrane domain (TMD) has been identified as an important region for transducing the chemical energy from agonist (e.g., GABA) binding in the ECD to gating of the channel pore in the TMD (Fig. 1) (15–19). Structurally, the M2-M3 linker moves radially outward along with the top of the pore-lining M2 helices during channel opening (20–22). However, the role of the M2-M3 linker in allosteric modulation by BZDs or the intrinsic energetics of the pore in the absence of agonist are less studied.

Previously we identified a specific residue, the central valine in the α1 subunit M2-M3 linker (V279), that regulates the efficiency of energetic linkage between diazepam (DZ) bound in the ECD and the pore gate in the TMD (23). Both functional and structural observations indicate that channel gating and allosteric modulation by BZDs involves conformational changes throughout the receptor (24–29) including changes in buried surface area at all intersubunit interfaces and with the M2-M3 linkers of all subunits undergoing a radial expansion during pore opening (20,21,30). Thus, we investigate here the effects of alanine substitutions in the analogous central position of α1(V279) in the M2-M3 linkers of β2 (I275A) and γ2 (V290A) subunits (Fig. 1). Specifically, we explore how these alanine substitutions affect the intrinsic closed-open equilibrium and linkage between DZ bound in the ECD and the pore gate in the TMD. Although DZ does also bind to several lower affinity sites in the TMD (20,21), the observed saturation of DZ responses in this study at 1–3 μM DZ suggests that we are primarily assaying binding to the high affinity site in the ECD (31). We show here that alanine substitution at the center of the M2-M3 linker has subunit-specific effects on the intrinsic closed-open equilibrium and its modulation by DZ.

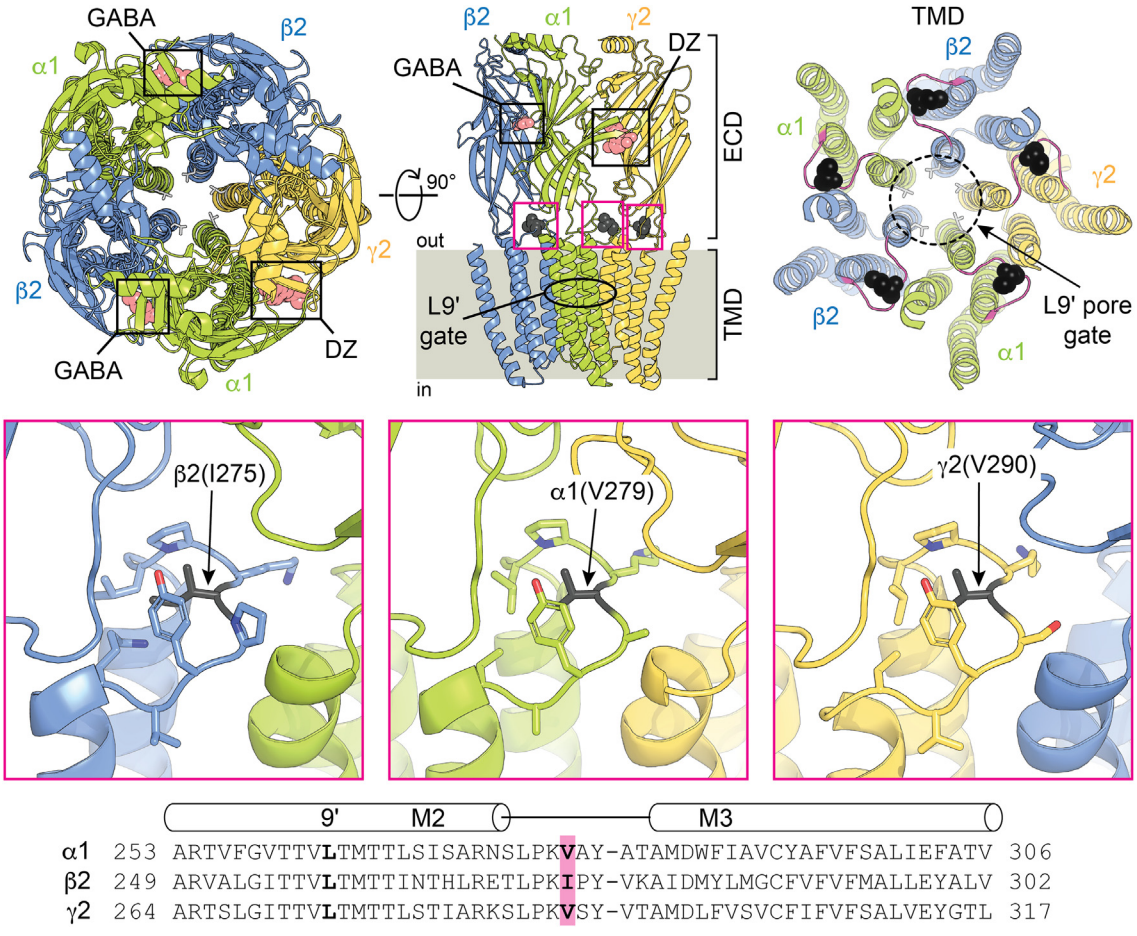

FIGURE 1 Cryo-EM structural representation of a synaptic $GABA_Aα1β2γ2$ receptor in complex with GABA and DZ. Upper left: top-down view from the extracellular side of the membrane. Subunits α1, β2, and γ2 are shown in green, blue, and yellow, respectively, with bound GABA and DZ as salmon spheres. The 9′ leucines forming the central pore gate are shown as light gray sticks. Upper middle: side-on view from the plane of the membrane omitting back two subunits for clarity. The central residue in each M2-M3 linker that was mutated in this study is shown as black spheres. Upper right: top-down view with the ECD removed and M2-M3 linkers colored magenta. Middle boxes: expanded views of the M2-M3 linker residues that were mutated in this study shown as black sticks. Location of each view corresponds to the magenta boxes in the upper middle panel. Cryo-EM map is from PDB: 6X3X. Note that rat α1(V279) corresponds to human α1(V280) in the cryo-EM map. Bottom: sequence alignment of M2-M3 linker regions in rat subunits. Mutation sites and 9′ leucines are highlighted.

Rationale for use of a gain-of-function mutant as a background on which to probe the intrinsic pore closed-open equilibrium and linkage between the BZD site and the pore gate

Weak modulatory drugs such as BZDs do not confer appreciable channel opening by themselves, but rather regulate the channel's response to an agonist such as GABA. Thus, electrophysiological measures of channel current necessitate coapplication of both drug and agonist to open the channel. This complicates elucidation of the molecular linkage between the drug site and the pore gate because 1) the agonist's energetic contribution to pore gating typically dominates compared with the weak modulator and 2) it is difficult to distinguish between direct effects of the modulator on the pore equilibrium versus indirect effects via a change in agonist affinity while the modulator is bound. To overcome these challenges and investigate the energetic linkage between the BZD site in the ECD and the pore gate in the TMD, we leverage the gain-of-function mutation α1(L9′T) in the M2 pore-lining helix (Fig. 1) (32–34). This mutation in the hydrophobic pore gate confers spontaneous exchange between closed and open states in the absence of ligand, to which changes in current in response to either BZDs or mutations can be readily detected. Thus, this mutant allows straightforward quantification of the energetic consequence of BZD binding or a mutation on the pore closed-open equilibrium from conventional measures of channel current (23).

Importantly, α1(L9′T)β2γ2 receptors exhibit the same pharmacology as wild-type receptors, being blocked by picrotoxin (PTX), allosterically modulated by BZDs, and activated robustly by GABA (Fig. 2) (33,34). Kinetic analysis of macroscopic currents elicited with rapid jumps in ligand concentration indicate that nearly all the effects of the α1(L9′T) mutation can be explained by a stabilization of the open conformation with little change to the energetics of closed or desensitized states (34). A similar conclusion based on both single channel recordings and macroscopic kinetic analyses was reached for the γ2(L9′S) gain-of-function mutation (35). This suggests that the primary effect of the α1(L9′T) mutation is to shift the intrinsic closed-open equilibrium while otherwise maintaining the same mechanism for gating and allosteric modulation as in wild-type channels, similar to observations of gain-of-function mutations in nicotinic acetylcholine receptors (36). If this is true, then activation of wild-type channels with lower concentrations of GABA that elicit similar activity to the gain-of-function mutant should be equivalent. However, whenever an agonist such as GABA is used to obtain a desired level of activity, it is difficult to distinguish between a mutation having a direct effect on the pore equilibrium versus an indirect effect via a change in agonist affinity (37). Thus, we chose to use the α1(L9′T) gain-of-function mutation for a uniform background on which to probe the energetics of the pore equilibrium and its linkage with the classical BZD site in the ECD without complication from any changes in agonist affinity. We note that we have shown previously (23) and show here that observations for mutations in the α1(L9′T) background have translated to predicted effects in wild-type channels.

MATERIALS AND METHODS

Mutagenesis and expression in oocytes

DNA for rat $GABA_AR$ α1, β2, and γ2 subunits were a gift from Dr. Cynthia Czajkowski. Note that the long isoform of γ2 was used throughout. The α1(L9′T) and α_m mutations were introduced individually or serially by site-specific mutagenesis (QuikChange II, QIAGEN, Redwood City, CA). Mutations β_m and γ_m were obtained from GENEWIZ (South Plainfield,

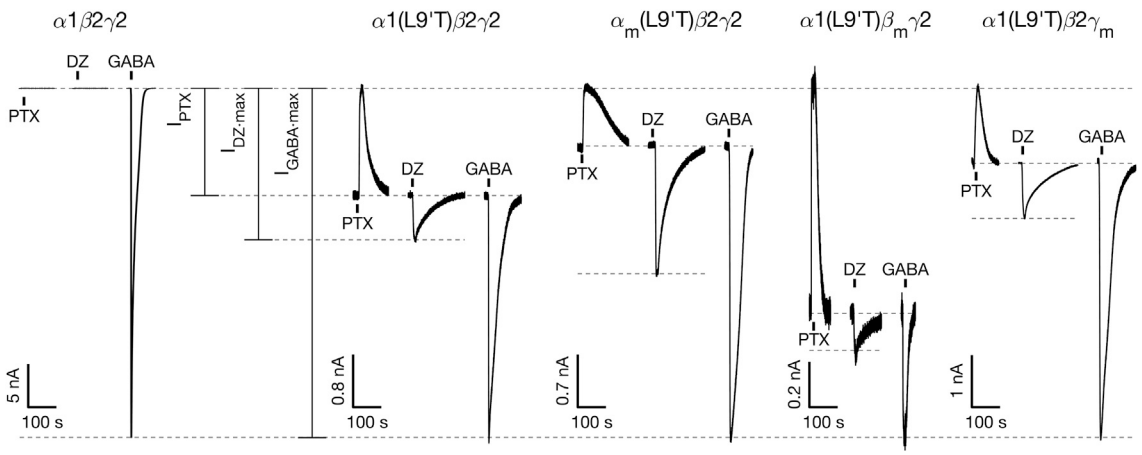

FIGURE 2 M2-M3 linker mutations α_m, β_m, or γ_m have subunit-specific effects on the intrinsic closed-open equilibrium and its modulation by DZ. Example currents from wild-type α1β2γ2 and gain-of-function α1(L9′T)β2γ2 receptors without and with M2-M3 linker mutations α_m, β_m, or γ_m. Currents are in response to 10 s pulses (*black bars*) of either 1 mM PTX, saturating 1–3 μM DZ (high affinity ECD site), or saturating GABA. Full concentration-response curves are shown in Figs. S1 and S2. Current block by the pore blocker PTX was used to assess the amount of spontaneous activity and to normalize DZ- and GABA-evoked responses from different oocytes. Currents are normalized from the zero-current baseline in PTX to the maximal GABA-evoked response.

NJ). Each construct was verified by forward and reverse sequencing of the entire gene.

For expression in *Xenopus laevis* oocytes (EcoCyte Bioscience, Austin, TX), cRNA for each construct was generated from DNA plasmids (mMessage mMachine T7, Ambion, Austin, TX). Oocytes were injected with 27–54 ng of total mRNA for α, β, and γ subunits (or mutants) in a 1:1:10 ratio (38) (Nanoject, Drummond Scientific, Broomall, PA). Oocytes were incubated in ND96 (in mM: 96 NaCl, 2 KCl, 1 MgCl2, 1.8 $CaCl_2$, 5 HEPES [pH 7.2]) with 100 mg/mL gentamicin at 18°C.

Two-electrode voltage-clamp recording and analysis

Currents from expressed channels 1–3 days postinjection were recorded using a two-electrode voltage clamp (Dagan TEV-200 amplifier, Minneapolis, MN, HEKA ITC digitizer and Patchmaster software, Holliston, MA). Oocytes were held at −80 mV and perfused continuously with buffer (ND96) or buffer containing PTX, GABA, or DZ. PTX was diluted from a 1 M stock solution in DMSO. DZ was diluted from a 10 mM stock solution in DMSO. Fresh PTX and DZ stock solutions were tested several times with no change in results. GABA was dissolved directly from powder. A microfluidic pump (Elveflow OB1 MK3+) and rotary valve (Elveflow MUX Distributor, Paris, France) provided consistent and repeatable perfusion and solution exchange across experiments, which limited solution exchange variability to primarily differences between oocytes only. Ten second pulses of PTX, GABA, or DZ were followed by 3–6 min in buffer to allow currents to return to baseline. Recorded currents were analyzed with custom scripts in MATLAB (The MathWorks, Natick, MA).

Recordings of concentration-response relationships were bookended by pulses of PTX to correct for any drift or rundown during the experiment and to identify the zero current baseline. As described previously (23), in some oocytes we accounted for a gradual rundown of channel current during the time course of the recording by applying a linear scaling in time so that the initial and final PTX responses were of equal amplitude. It is worth noting that such scaling had little to no effect on the ratio of the maximal GABA- or DZ-evoked responses ($I_{GABA\cdot max}$ or $I_{DZ\cdot max}$) to the following final PTX response (I_{PTX}) as used to estimate open probability and conferred only minor shifts at most to the concentration-response relationships. The amount of current rundown was variable across oocytes, with no clear relation to specific constructs.

Current (I) concentration-response curves (CRCs) were measured with respect to the unliganded current baseline and fit to the Hill equation:

$$I = \frac{I_{max}}{1 + \left(\frac{EC_{50}}{[X]}\right)^{h}} \quad (1)$$

where I_{max} is the peak current response relative to the unliganded current baseline, $[X]$ is ligand concentration, EC_{50} is the concentration eliciting a half-maximal response, and h is the Hill coefficient. Note that, although the parameters from Hill fits provide a general metric for assessing apparent affinity and sensitivity, they are not easily translatable into physical parameters such as affinities of specific sites or numbers of bound ligands (39,40).

DZ-gating model

The DZ-gating model (Fig. 5 *A*) is the same as described previously (23). In brief, the free energy difference from closed to open states was calculated for unliganded ($\Delta G_{unliganded}$) or DZ-bound ($\Delta G_{DZ\cdot bound}$) receptors as follows:

$$\Delta G_{unliganded} = -RT\, ln\left(\frac{P_{o\cdot unliganded}}{1 - P_{o\cdot unliganded}}\right) \quad (2)$$

$$\Delta G_{DZ\cdot bound} = -RT\, ln\left(\frac{P_{o\cdot DZ\cdot bound}}{1 - P_{o\cdot DZ\cdot bound}}\right) \quad (3)$$

where RT is the product of the gas constant and temperature, and we estimated $P_{o\cdot unliganded} \approx I_{PTX}/I_{GABA\cdot max}$ and $P_{o\cdot DZ\cdot bound} \approx I_{DZ\cdot max}/I_{GABA\cdot max}$. This estimate is reasonable for gain-of-function mutants whose open probability in saturating GABA is close to one. See Fig. 2 for an illustration of I_{PTX}, $I_{DZ\cdot max}$, and $I_{GABA\cdot max}$. The energetic consequence of DZ binding on the pore closed-open equilibrium $\Delta\Delta G_{DZ}$ is the difference between DZ-bound and unliganded conditions:

$$\Delta\Delta G_{DZ} = \Delta G_{DZ\cdot bound} - \Delta G_{unliganded} \quad (4)$$

RESULTS

Effects of alanine substitutions in the center of the M2-M3 linkers of specific subunits on GABA- and DZ-evoked currents in a gain-of-function receptor

We previously identified a specific residue in the center of the α1 subunit M2-M3 linker (rat V279, human V280) that is involved in mediating linkage between the BZD DZ and the pore gate (23). Here, we investigate the effects of alanine substitutions at the analogous central positions in the M2-M3 linkers of rat α1, β2, and γ2 subunits in wild-type α1β2γ2 and gain-of-function α1(L9′T)β2γ2 $GABA_A$Rs (α_m = α1(V279A); β_m = β2(I275A); γ_m = γ2(V290A)). Note that rat and human sequences are nearly identical, differing by only one residue in α1 and β2 subunits in disordered regions at the N-terminus or in the M3-M4 intracellular linker, respectively, and in γ2 subunits having slightly different lengths of M3-M4 linkers. *Xenopus laevis* oocytes were coinjected with mRNA for α1, β2, and γ2 subunits (or mutants) in a 1:1:10 ratio (38), and current responses to microfluidic application of ligands were recorded using a two-electrode voltage clamp. Activation by DZ indicates incorporation of the γ2 subunit, and we further assume that all constructs assemble primarily with the canonical $(\alpha)_2(\beta)_2(\gamma)_1$ stoichiometry (41).

For wild-type α1β2γ2 receptors, no detectable currents were evoked upon application of the pore blocker PTX or the weak modulator DZ, whereas robust currents were elicited with GABA (Fig. 2). These observations are as expected for channels that are closed at rest and consistent with DZ being a sufficiently weak modulator that it is unable to open the pore to an observable level on its own. In contrast, receptors harboring the gain-of-function α1(L9′T) mutation exhibited both spontaneous PTX-sensitive current (I_{PTX}) and additional current beyond the spontaneous current baseline in response to DZ alone (I_{DZ}) (Fig. 2). The ability of DZ to elicit increased channel activity in the gain-of-function mutant parallels its ability to potentiate responses to subsaturating concentrations of agonist (e.g., GABA) in wild-type receptors (42) and illustrates that DZ does energetically bias the pore toward an open conformation. This bias is insufficient to observe

channel opening in wild-type receptors but is readily detected in the gain-of-function mutant with a much smaller energy difference between closed and open conformations.

For each oocyte we recorded current responses to a series of 10 s pulses of increasing concentrations of either GABA or DZ bookended by 10 s pulses of 1 mM PTX (Figs. S1-2). Current block by the pore blocker PTX was used to assess the amount of spontaneous unliganded activity (I_{PTX}) and to define the zero current baseline. For comparison across oocytes, currents were normalized from the zero current baseline in PTX to the maximal GABA-evoked response ($I_{GABA\cdot max}$) (Fig. 2). For DZ recordings lacking a response to saturating GABA, currents were normalized such that the PTX-sensitive current amplitude in the DZ recording matched the median PTX-sensitive current amplitude across normalized GABA recordings for the same construct. This amounts to computing the fold-increase in basal open probability conferred by DZ. GABA and DZ CRCs were computed for ligand-evoked current amplitudes with respect to the unliganded current baseline (i.e., the baseline current in the absence of any ligands) and fit to the Hill equation (Eq. 1 in materials and methods; Figs. S1–S8). For each construct, the GABA or DZ CRCs were pooled after normalizing to their individual Hill fits, and the pooled data were fit to the Hill equation with $I_{max} = 1$. Importantly, no currents were elicited upon application of PTX, GABA, or DZ in uninjected oocytes (data not shown).

The gain-of-function mutant α1(L9′T)β2γ2 left-shifts the GABA CRC by ∼100-fold, consistent with previous reports (33) and qualitatively as expected for a bias from closed to open conformations where GABA binds with higher affinity to open versus closed states (Fig. S7). In the α1(L9′T)β2γ2 background, the individual mutations α_m or γ_m had little effect on GABA CRCs, whereas β_m right-shifted the CRC by ∼10-fold and conferred a reduced sensitivity with a Hill coefficient less than one (Figs. S4 and S7). Thus, β_m contributes to apparent affinity for GABA binding, whereas α_m and γ_m do not. None of the individual mutations α_m, β_m, or γ_m had any effect on DZ CRCs (Figs. S5 and S8), indicating that the mutations do not appreciably perturb affinity for DZ binding. Reports for the EC_{50} of DZ-potentiation in wild-type receptors are comparable with the observed EC_{50} for direct DZ-gating of gain-of-function receptors reported here and in previous studies (Fig. S8) (23,31,33,43,44).

Asymmetric roles for the central residue of the M2-M3 linker of specific subunits in regulating the pore closed-open equilibrium

The spontaneous unliganded open probability ($P_{o\cdot unliganded}$) is given by the product of the maximal open probability in saturating GABA ($P_{o\cdot GABA\cdot max}$) and the ratio of the PTX-sensitive to the maximal GABA-evoked current amplitudes ($I_{PTX}/I_{GABA\cdot max}$ as shown in Fig. 2). For wild-type α1β2γ2 receptors, $P_{o\cdot GABA\cdot max} \approx 0.8$ (45). Under the assumption that all gain-of-function constructs (e.g., constructs harboring the α1(L9′T) mutation) should increase $P_{o\cdot GABA\cdot max}$ to something approaching one, we estimate for these constructs $P_{o\cdot unliganded} \approx I_{PTX}/I_{GABA\cdot max}$ (ratios are of absolute current amplitudes as defined in Fig. 2). We previously verified from single-channel recordings that $P_{o\cdot GABA\cdot max} = 0.93$ for α_m(L9′T)β2γ2 receptors (23). Importantly, our primary conclusions are relatively insensitive to such small errors in the estimation of $P_{o\cdot GABA\cdot max}$.

In the α1(L9′T)β2γ2 background, both α_m and γ_m reduced the unliganded open probability by ∼2-fold (Fig. 3). In contrast, β_m increased the spontaneous unliganded open probability by ∼2- to ∼0.7-fold which is close to the maximal open probability in saturating GABA for wild-type receptors (Fig. 3). Thus, mutation of the central residue in the β2 subunit M2-M3 linker from isoleucine to alanine dramatically increases the intrinsic probability of pore opening, whereas the analogous mutations in the α1 or γ2 subunits inhibit spontaneous unliganded activity.

Given the large increase in intrinsic open probability conferred by β_m in the α1(L9′T)β2γ2 background, we asked whether β_m provides a sufficient bias for an open conformation to detect appreciable unliganded channel opening in the absence of the gain-of-function α1(L9′T) mutation. To test this, we repeated the same PTX and GABA concentration-response protocol described above for α1β_mγ2 receptors (Figs. 4 *A* and S3). The clear PTX-sensitive current verifies that β_m alone is sufficient to open the channel pore in the absence of ligand. In contrast, α_mβ2γ2 receptors did not exhibit any obvious PTX-sensitive current, as expected given that α_m reduces spontaneous activity in the α1(L9′T)β2γ2 background (Figs. 4 *A* and S3). We did not test γ_m as it also reduces spontaneous activity similar to α_m. Consistent with α_m inhibiting and β_m promoting intrinsic pore opening, in the wild-type α1β2γ2 background α_m or β_m right- or left-shifted

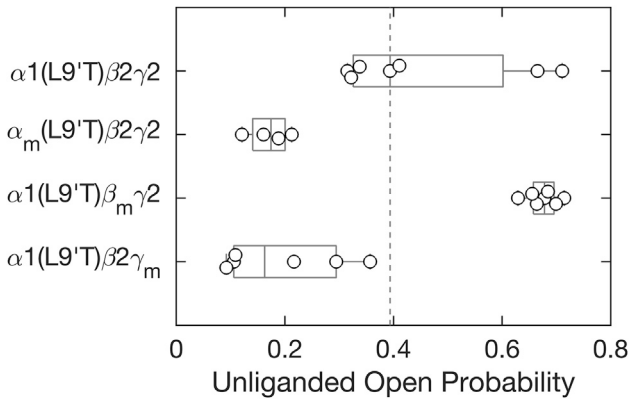

FIGURE 3 M2-M3 linker mutations either enhance (β_m) or inhibit (α_m, γ_m) intrinsic pore opening in the absence of ligand. Spontaneous open probability for M2-M3 linker mutations α_m, β_m, or γ_m in the background of the gain-of-function mutation α1(L9′T) estimated as the ratio of PTX-sensitive to maximal GABA-evoked current amplitudes $I_{PTX}/I_{GABA\cdot max}$ (see Fig. 2). Data points are for individual oocytes (α1(L9′T)β2γ2: $n = 7$; α_m(L9′T)β2γ2: $n = 4$; α1(L9′T)β_mγ2: $n = 7$; α1(L9′T)β2γ_m: $n = 6$). Boxplots indicate quartiles, and the vertical dashed line is the median for the α1(L9′T)β2γ2 background.

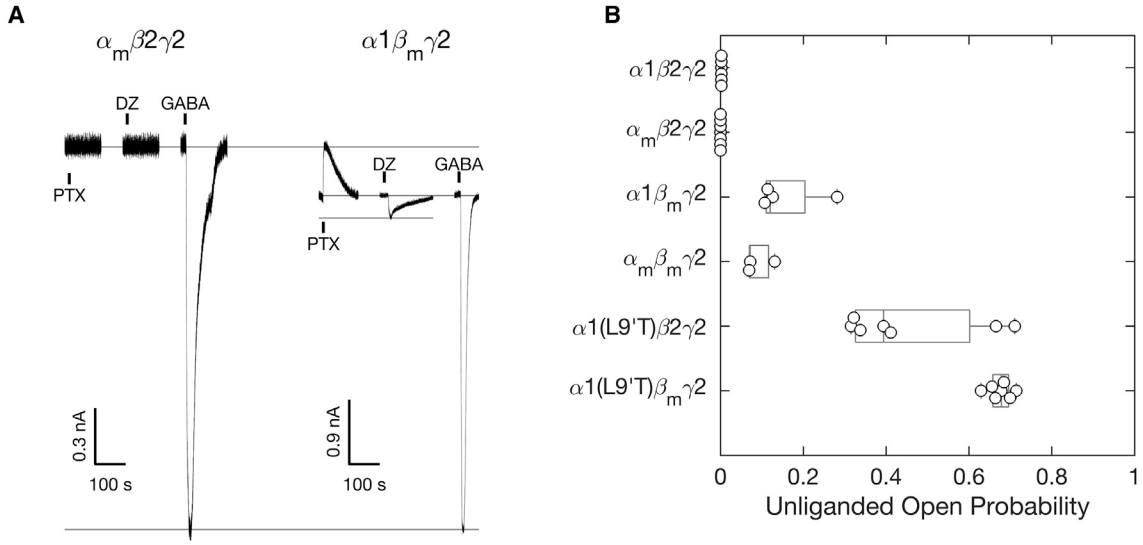

FIGURE 4 The central residue (I275) in the β2 subunit M2-M3 linker is required to keep the channel closed in the absence of ligand. (*A*) Example currents from receptors with α_m or β_m mutations in a wild-type $\alpha1\beta2\gamma2$ background. Currents are in response to 10 s pulses (*black bars*) of either 1 mM PTX, saturating 3 μM DZ (high affinity ECD site), or saturating GABA. Full concentration-response curves are shown in Fig. S3. Current block by the pore blocker PTX was used to assess the amount of spontaneous activity and to normalize DZ- and GABA-evoked responses from different oocytes. Currents are normalized from the zero-current baseline in PTX to the maximal GABA-evoked response. (*B*) Spontaneous unliganded open probability for M2-M3 linker mutations α_m and/or β_m in wild-type $\alpha1\beta2\gamma2$ and gain-of-function $\alpha1$(L9′T)$\beta2\gamma2$ backgrounds estimated as the ratio of PTX-sensitive to maximal GABA-evoked current amplitudes $I_{PTX}/I_{GABA\cdot max}$ (see (*A*) and Fig. 2). Data points for constructs including the $\alpha1$(L9′T) mutation are as shown in Fig. 3. Data points are for individual oocytes ($\alpha1\beta2\gamma2$: $n = 6$; $\alpha_m\beta2\gamma2$: $n = 7$; $\alpha1\beta_m\gamma2$: $n = 4$; $\alpha_m\beta_m\gamma2$: $n = 3$; $\alpha1$(L9′T)$\beta2\gamma2$: $n = 7$; $\alpha1$(L9′T)$\beta_m\gamma2$: $n = 7$). Boxplots indicate quartiles.

GABA CRCs, respectively (Figs. S6-7). Given that β_m is a gain-of-function mutation, we estimated the unliganded open probability in the same manner as for channels with the $\alpha1$(L9′T) mutation. In comparison to $\alpha1$(L9′T)$\beta2\gamma2$, $\alpha1\beta_m\gamma2$ receptors were open spontaneously approximately half as much, whereas the combination of both mutations in $\alpha1$(L9′T)$\beta_m\gamma2$ receptors conferred the most unliganded channel opening, consistent with effects of the gain-of-function mutations $\alpha1$(L9′T) and β_m being at least partially additive and independent (Fig. 4 *B*). However, see below in the section on combinations of mutations for their nonadditive energetic effects on the intrinsic closed-open equilibrium.

These data show that the central position in the β2 subunit M2-M3 linker is important for regulating the intrinsic closed-open equilibrium in $GABA_A$ receptors. Unlike $\alpha1$(L9′T), β_m (I275A) is located outside of the pore, suggesting that this regulation may overlap with events underlying the transduction of the chemical energy from ligand binding to pore gating. In contrast, alanine substitutions at the analogous position in the M2-M3 linker of α1 or γ2 inhibit pore opening, indicating an asymmetric role for specific subunit M2-M3 linkers in regulating the pore closed-open equilibrium.

Asymmetric roles for the central residue of the M2-M3 linker of specific subunits in regulating the efficiency of DZ-to-pore linkage

Despite having little effect on DZ apparent affinity, we previously identified that the α_m mutation increases the efficiency of transduction of chemical energy from DZ binding to gating of the channel pore by up to threefold (23). Intriguingly, this increase in DZ efficiency was only observed for alanine substitution at the central residue (V279) of the rat α1 subunit M2-M3 linker, whereas alanine substitutions at other residues in the linker had no effect (23). In addition to its high affinity site in the ECD (Fig. 1), DZ also binds to several lower-affinity sites in the TMD (20,21). However, the observed saturation of DZ responses in this study at 1–3 μM DZ suggests that we are primarily assaying binding to the high affinity site in the ECD (31). Thus, we interpret our results as probing linkage between the high-affinity BZD site in the ECD and the pore gate in the TMD.

Given that structural changes conferred upon DZ binding appear to involve global changes in conformation with similar gross overall changes in each subunit (20,21), as well as functional evidence that BZDs confer global conformational changes at multiple subunit-subunit interfaces (24–29), we asked whether the analogous alanine substitutions at the center of the M2-M3 linkers in β2 or γ2 subunits would confer similar effects on DZ efficiency. We employed a simple channel gating scheme between closed (C) and open (O) pore states in both unliganded and DZ-bound conditions to quantify the energetic linkage between DZ binding and pore gating (Fig. 5 *A*). In the absence or presence of DZ we estimated the maximal unliganded or DZ-evoked open probability as either $P_{o\cdot unliganded} = I_{PTX}/I_{GABA\cdot max}$ or $P_{o\cdot DZ\cdot bound} = I_{DZ\cdot max}/I_{GABA\cdot max}$ (ratios are of absolute current amplitudes as defined in Fig. 2). The free energy

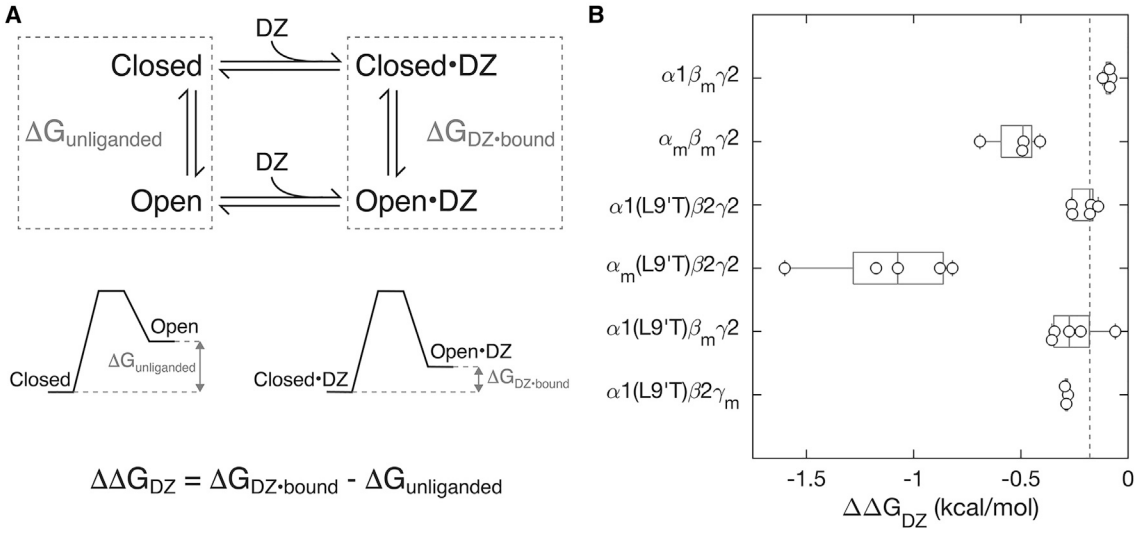

FIGURE 5 The α1 subunit M2-M3 linker mutation α_m enhances DZ modulation of pore gating, whereas analogous mutations in β2 or γ2 subunits have little effect. (*A*) Simple scheme for gating between closed and open conformations (*vertical arrows*) with DZ binding and unbinding (*horizontal arrows*) separating unliganded and DZ-bound states. The free energy difference between open and closed conformations in both unliganded ($\Delta G_{unliganded}$) and DZ-bound ($\Delta G_{DZ\cdot bound}$) conditions are depicted graphically below the scheme. See Eqs. 2 and 3 in materials and methodsfor how these energies are computed. (*B*) The change in closed versus open free energies upon DZ binding in the ECD (see Eq. 4 in materials and methods) for α_m, β_m, or γ_m mutations in wild-type α1β2γ2 and/or gain-of-function α1(L9′T)β2γ2 backgrounds. The more negative the value of $\Delta\Delta G_{DZ}$, the more DZ increases channel open probability. Data points are for individual oocytes (α1β_mγ2: $n = 4$; $\alpha_m\beta_m\gamma2$: $n = 4$; α1(L9′T)β2γ2: $n = 5$; α_m(L9′T)β2γ2: $n = 5$; α1(L9′T)β_mγ2: $n = 5$; α1(L9′T)β2γ_m: $n = 3$). Boxplots indicate quartiles, and the vertical dashed line is the median for the α1(L9′T)β2γ2 background.

difference between closed and open states in unliganded ($\Delta G_{unliganded}$) or DZ-bound ($\Delta G_{DZ\cdot bound}$) conditions is given by Eqs. 2 and 3 (see materials and methods). The energetic consequence of DZ binding on the pore closed-open equilibrium is the difference between DZ-bound and unliganded conditions: $\Delta\Delta G_{DZ} = \Delta G_{DZ\cdot bound} - \Delta G_{unliganded}$.

In contrast to our previous observation that α_m increases the energetic linkage between DZ binding and pore gating (23), we observe little to no effect of the analogous mutations β_m or γ_m on $\Delta\Delta G_{DZ}$ (Fig. 5 *B*). These data suggest that linkage between DZ binding and the pore gate is mediated differentially by M2-M3 linkers of specific subunits.

Combinations of M2-M3 linker mutations with subunit-specific effects

To assess the independence of α_m, β_m, and γ_m mutations we measured GABA and DZ CRCs, spontaneous unliganded open probabilities, and DZ-to-pore linkage energetics for combinations of mutations in the α1β2γ2 and α1(L9′T)β2γ2 backgrounds in the same manner as for the individual mutations. In the α1(L9′T)β2γ2 background, all double mutants and the triple mutant right-shifted GABA CRCs by ∼3- to 10-fold with either similar or increased sensitivities, i.e., Hill coefficients (Figs. S4 and S7). Interestingly, every subunit combination that includes the β_m mutation exhibits a similar GABA EC_{50} independent of whether the α1(L9′T) mutation is present. If the shifts in GABA EC_{50} reflect only the degree of bias toward the higher-affinity open conformation, then the combination of α1(L9′T) and β_m should be even more left-shifted than either mutation alone. However, we observe a right-shift in GABA EC_{50} for α1(L9′T)β_mγ2 as compared with α1(L9′T)β2γ2, suggesting that β_m has a dominant effect on setting the affinity for GABA binding in the ECD in addition to its effect on the intrinsic pore equilibrium. In contrast, nearly all combinations of α_m, β_m, and γ_m mutations had little effect on DZ CRCs, like observations for the individual mutations, the exception being a fourfold right-shift in the DZ EC_{50} for $\alpha_m\beta_m\gamma2$ (Figs. S5, S6 *B*, and S8).

For nearly all tested combinations of mutations, the intrinsic probability of spontaneous unliganded pore opening was enhanced by β_m and inhibited by α_m and/or γ_m (Fig. 6). The only exception is that α1(L9′T)$\beta_m\gamma_m$ receptors exhibit similar or even more spontaneous activity than α1(L9′T)β_mγ2 receptors, despite the addition of γ_m. The reason for this exception is not clear. The combination of β_m and α1(L9′T) conferred a spontaneous unliganded open probability that was roughly the sum of the spontaneous open probabilities for each of the individual mutations. However, the effect of the individual mutations β_m and α1(L9′T) on the free energy difference between closed and open states in the absence of ligand ($\Delta G_{unliganded}$) are not additive. For wild-type α1β2γ2 receptors we estimate $P_{o\cdot unliganded} = 0.002$(46), from which Eq. 2 (see materials and methods) implies $\Delta G_{unliganded} = 3.7$ kcal/mol. Either β_m or α1(L9′T) reduce $\Delta G_{unliganded}$ to 1.0 or 0.1 kcal/mol, respectively, thereby increasing the probability of spontaneous channel opening. However, for the combination of both mutations in α1(L9′T)β_mγ2 receptors $\Delta G_{unliganded} = -0.3$ kcal/mol, which is only slightly less than for

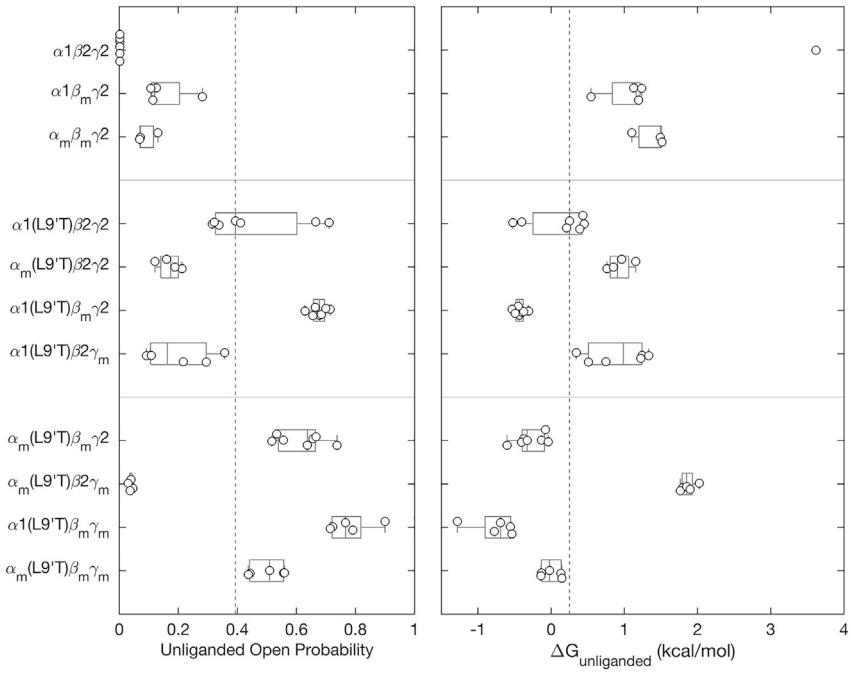

FIGURE 6 M2-M3 linker mutations either enhance (β_m) or inhibit (α_m, γ_m) intrinsic pore opening in the absence of ligand. Left: spontaneous unliganded open probability for receptors with M2-M3 linker mutations α_m, β_m, and/or γ_m in the gain-of-function $\alpha1(L9'T)\beta2\gamma2$ or wild-type $\alpha1\beta2\gamma2$ backgrounds estimated as the ratio of PTX-sensitive to maximal GABA-evoked current amplitudes (see Figs. 2 and 4). Right: free energy difference from closed to open states calculated from the unliganded open probability using Eq. 2 (see materials and methods). $\Delta G_{unliganded}$ for $\alpha1\beta2\gamma2$ receptors is based on the estimate $P_{o\cdot unliganded} = 0.002$ (46), which is undetectable in our assay. All other data points are for individual oocytes ($\alpha1\beta2\gamma2$: $n = 6$; $\alpha1\beta_m\gamma2$: $n = 4$; $\alpha_m\beta_m\gamma2$: $n = 3$; $\alpha1(L9'T)\beta2\gamma2$: $n = 7$; $\alpha_m(L9'T)\beta2\gamma2$: $n = 4$; $\alpha1(L9'T)\beta_m\gamma2$: $n = 7$; $\alpha1(L9'T)\beta2\gamma_m$: $n = 6$; $\alpha_m(L9'T)\beta_m\gamma2$: $n = 7$; $\alpha_m(L9'T)\beta2\gamma_m$: $n = 5$; $\alpha1(L9'T)\beta_m\gamma_m$: $n = 5$; $\alpha_m(L9'T)\beta_m\gamma_m$: $n = 5$). Boxplots indicate quartiles, and the vertical dashed line is the median for the $\alpha1(L9'T)\beta2\gamma2$ background. The unliganded open probabilities for some of the constructs are the same as shown in Figs. 3 and 4.

$\alpha1(L9'T)$ alone. Thus, the effects of β_m outside of the pore and $\alpha1(L9'T)$ at the pore gate on the channel's closed-open equilibrium are energetically nonindependent. It seems plausible that both mutations may promote similar conformational changes to enhance channel opening.

In the $\alpha1(L9'T)\beta2\gamma2$ background the combination of α_m and γ_m on $\Delta G_{unliganded}$ was roughly the sum of the effects of the individual mutations (Fig. 6). Thus, inhibition of pore opening by α_m and γ_m is largely independent. In contrast, $\Delta G_{unliganded}$ for combinations of either α_m or γ_m with β_m was similar to that for β_m alone. This indicates that the enhancement of channel gating conferred by β_m largely dominates such that α_m or γ_m can no longer confer their inhibitory effects. Thus, whereas α_m and γ_m are largely independent of each other, they are not independent of β_m. However, in the triple mutant $\alpha_m(L9'T)\beta_m\gamma_m$ the combination of both α_m and γ_m is sufficient to slightly inhibit the gain-of-function conferred by β_m.

DZ-to-pore linkage $\Delta\Delta G_{DZ}$ in the triple mutant $\alpha_m(L9'T)\beta_m\gamma_m$ was much smaller in magnitude than expected based on energetic additivity of the individual mutations, indicating that the mutations are not independent (Fig. 7). The double mutants $\alpha_m(L9'T)\beta_m\gamma2$ and $\alpha_m(L9'T)\beta2\gamma_m$ also exhibited $\Delta\Delta G_{DZ}$ values that appear slightly less than additive, although the variation in the data makes it difficult to determine this unambiguously. However, the qualitative observation that α_m enhances the efficiency of DZ-gating remains true when in combination with either β_m or γ_m in the $\alpha1(L9'T)\beta2\gamma2$ background, and with β_m in the $\alpha1\beta2\gamma2$ background. In the $\alpha1(L9'T)\beta2\gamma2$ background this enhancement is, if anything, reduced when α_m is combined with either β_m or γ_m, and is reduced appreciably for the combination of all three mutations α_m, β_m, and γ_m. The mechanism for the nonadditive effects of combinations of mutations on $\Delta\Delta G_{DZ}$ is unclear but indicates that it is at least possible for M2-M3 linkers from each subunit to contribute to DZ-to-pore linkage.

DISCUSSION

We show that alanine substitutions at the central residue in the M2-M3 linkers of specific subunits α_m, β_m, or γ_m have asymmetric effects on the intrinsic unliganded closed-open equilibrium and its modulation by DZ. Whereas α_m and γ_m inhibit pore opening, β_m promotes opening to the extent that this mutation alone is sufficient to cause the channel to open spontaneously in the absence of agonist. Estimating the unliganded open probability in wild-type $\alpha1\beta2\gamma2$ receptors as 0.002 (46), the energetic effect of β_m on the closed-open equilibrium is −2.5 kcal/mol (using Eq. 2 in materials and methods), which is more than half the −4.5 kcal/mol supplied by GABA binding to the two neurotransmitter sites (i.e., for a change in open probability from 0.002 to 0.8). In contrast, only α_m increases the efficiency of DZ-to-pore linkage, whereas β_m or γ_m have no effect. Summary statistics are shown in Table 1.

In this study we restrict our analysis to the relative populations of closed (nonconducting) versus open (conducting) channels. Although stabilization of the open state in spontaneously active mutants should minimize the effects of desensitization on the peak current responses (34), some residual desensitization coupled with the relatively slow solution exchange over the oocyte membrane may contribute to the

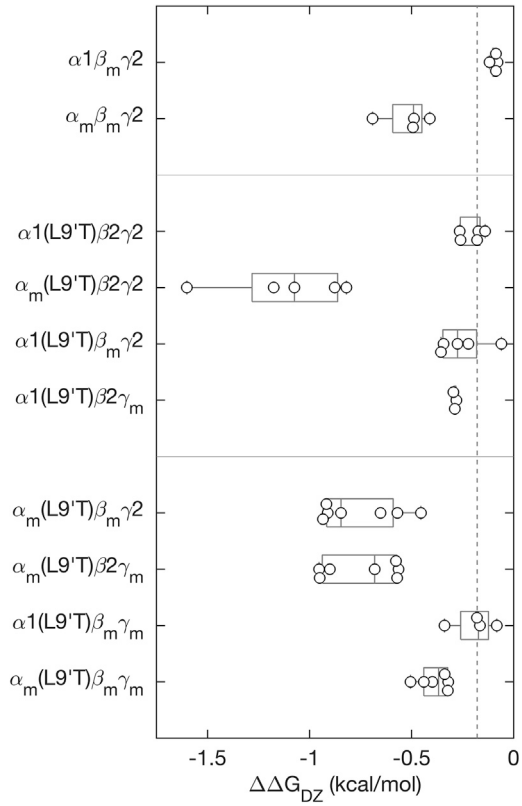

FIGURE 7 M2-M3 linker mutations either enhance (α_m) or have no effect (β_m, γ_m) on the energy DZ-binding in the ECD provides to the channel's closed-open equilibrium. The change in the free energy difference from closed to open states upon DZ binding in the ECD (see Eq. 4 in materials and methods) for α_m, β_m, or γ_m mutations in wild-type $\alpha1\beta2\gamma2$ and/or gain-of-function $\alpha1(L9'T)\beta2\gamma2$ backgrounds. The more negative the value of $\Delta\Delta G_{DZ}$, the more DZ increases channel open probability. Data points are for individual oocytes ($\alpha1\beta_m\gamma2$: $n = 4$; $\alpha_m\beta_m\gamma2$: $n = 4$; $\alpha1(L9'T)\beta2\gamma2$: $n = 5$; $\alpha_m(L9'T)\beta2\gamma2$: $n = 5$; $\alpha1(L9'T)\beta_m\gamma2$: $n = 5$; $\alpha1(L9'T)\beta2\gamma_m$: $n = 3$; $\alpha_m(L9'T)\beta_m\gamma2$: $n = 7$; $\alpha_m(L9'T)\beta2\gamma_m$: $n = 7$; $\alpha1(L9'T)\beta_m\gamma_m$: $n = 4$; $\alpha_m(L9'T)\beta_m\gamma_m$: $n = 6$). Boxplots indicate quartiles, and the vertical dashed line is the median for the $\alpha1(L9'T)\beta2\gamma2$ background. The data for some of the constructs are the same as shown in Fig. 5 *B*.

variation in our measurements. Ultimately, measures that can discern the kinetics of distinct states (e.g., resting-closed versus desensitized-closed) such as single-channel or excised patch recordings will likely be needed to address this question.

Comparison of $GABA_AR$ and other pLGIC structures in closed antagonist-bound and activated/desensitized agonist-bound conformations suggests that gating involves grossly symmetric motions of all five subunits including a radial expansion of the M2 pore lining helices and M2-M3 linkers (22,47). Similarly, comparison of $GABA_AR$ structures with and without BZDs suggest that BZDs such as DZ confer a global compaction of the ECD with increased intersubunit contacts, although the observed conformational changes are not large and differ in magnitude based on the solubilization strategy (20,21). However, all structures with bound BZD to-date were obtained in the presence of bound GABA where the complex with GABA is expected to energetically dominate the observed conformation. As discussed above, GABA binding to both agonist sites confer approximately −4.5 kcal/mol to channel gating compared with −0.4 kcal/mol for DZ in the ECD site (23). Furthermore, the observed effect of DZ decreases with increasing baseline activity, similar to recent observations for the energetic effect of the anesthetic propofol and neurosteroid etiocholanolone on the closed/open equilibrium (48). Indeed, functional studies show that DZ fails to potentiate responses to saturating GABA (49–53), suggesting that the presence of GABA may occlude the conformational effects of DZ in these structures. Nonetheless, there is also functional evidence for more global effects of BZDs on intersubunit interfaces throughout the receptor (24–29). Indeed, the nonadditive effects of various combinations of the mutations examined here indicate some cooperativity between the M2-M3 linkers of all subunits consistent with a global conformational change. However, the effects of individual mutations α_m, β_m, or γ_m are highly asymmetric.

We hypothesize that the decreased sidechain volume upon substitution of the central linker residue with alanine (α_m, β_m, γ_m) removes steric packing in the center of the roughly arc-shaped structure that the linker adopts and thereby confers an increase in linker flexibility (Fig. 1). Our previous observation that neither $\alpha1$(V297W) nor $\alpha1$(V297D) enhance DZ-to-pore linkage as does $\alpha1$(V297A) is consistent with this idea (23). However, it is unclear as to why increased flexibility in the M2-M3 linker of different subunits confers such disparate effects. A cryo-EM structural model of $\alpha1\beta3\gamma2$ receptors suggests that the domain including the M2-M3 linker and top of the M2 and M3 helices may be intrinsically more flexible in β2/3 subunits than in $\alpha1$ or $\gamma2$ subunits due to differential stabilization via intrasubunit interactions with a conserved 19′ arginine near the top of the M2 helix (21). A similar orientation of R19′ in one of the β subunits as compared with the other subunits was found in a recent structure of a native receptor from mouse brain (54). Changes in linker flexibility and intersubunit contacts have also been associated with closed versus open conformations of glycine receptors (55). Thus, a difference in intrinsic flexibility may contribute to the disparate effects of α_m, β_m, or γ_m on the closed-open equilibrium. However, the opposing effects of β_m as compared with α_m or γ_m on pore opening suggests that linker flexibility does not automatically map to increased channel activity but depends on the intersubunit interface in which the linker is located.

Changes in M2-M3 linker flexibility could also alter the overall compaction of the TMD helices thought to affect coupling with the BZD site (20). The observation that only α_m enhances the efficiency of DZ-to-pore linkage whereas β_m or γ_m does not suggests that the effects of the mutations on TMD compaction are either 1) global but opposing, 2) more localized to their respective intersubunit interfaces, or 3) not relevant. The idea of distinct effects at specific subunit-subunit interfaces is interesting

TABLE 1 Summary of the estimated unliganded open probability ($P_{o\cdot unliganded}$) and associated closed-open free energy difference ($\Delta G_{unliganded}$), DZ-to-pore linkage ($\Delta\Delta G_{DZ}$), and EC_{50} values for GABA and DZ CRCs for all tested constructs, values are median (25–75% interquartile range) across cells

	$P_{o\cdot unliganded}$	$\Delta G_{unliganded}$ (kcal/mol)	$\Delta\Delta G_{DZ}$ (kcal/mol)	GABA EC_{50} (μM)	DZ EC_{50} (μM)
α1β2γ2	0[a]	N/A	N/A	48 (32–65)	N/A
α_mβ2γ2	0[a]	N/A	N/A	410 (220–450)	N/A
α1β_mγ2	0.12 (0.11–0.20)	1.2 (0.9–1.2)	−0.1 (−0.1–(−0.1))	1.2 (1.1–1.3)	0.09 (0.06–0.11)
$\alpha_m\beta_m$γ2	0.07 (0.07–0.12)	1.5 (1.2–1.5)	−0.5 (−0.6–(−0.5))	16 (14–21)	0.34 (0.25–0.42)
α1(L9′T)β2γ2	0.39 (0.33–0.60)	0.3 (−0.3–0.4)	−0.2 (−0.3–(−0.2))	0.24 (0.18–0.37)	0.07 (0.06–0.10)
α_m(L9′T)β2γ2	0.17 (0.14–0.20)	0.9 (0.8–1.1)	−1.1 (−1.3–(−0.9))	0.28 (0.19–0.50)	0.12 (0.07–0.19)
α1(L9′T)β_mγ2	0.68 (0.66–0.70)	−0.4 (−0.5–(−0.4))	−0.3 (−0.4–(−0.2))	2.4 (2.0–2.6)	0.13 (0.07–0.17)
α1(L9′T)β2γ_m	0.16 (0.11–0.29)	1.0 (0.5–1.3)	−0.3 (−0.3–(−0.3))	0.27 (0.25–0.28)	0.07 (0.07–0.09)
α_m(L9′T)β_mγ2	0.64 (0.54–0.66)	−0.3 (−0.4–(−0.1))	−0.9 (−0.9–(−0.6))	1.7 (1.1–2.3)	0.11 (0.08–0.12)
α_m(L9′T)β2γ_m	0.04 (0.04–0.04)	1.9 (1.8–2.0)	−0.7 (−0.9–(−0.6))	0.58 (0.47–0.66)	0.25 (0.13–0.26)
α1(L9′T)$\beta_m\gamma_m$	0.77 (0.72–0.82)	−0.7 (−0.9–(−0.6))	−0.2 (−0.3–(−0.1))	0.62 (0.39–0.92)	0.13 (0.09–0.17)
α_m(L9′T)$\beta_m\gamma_m$	0.51 (0.44–0.56)	0.0 (−0.1–0.1)	−0.4 (−0.4–(−0.3))	1.1 (0.5–2.3)	0.06 (0.02–0.10)

Data for individual cells are plotted in Figs. 6, 7, S7, and S8.
[a]No detectable PTX-sensitive current.

given that the M2-M3 linkers in β subunits are located at the β/α intersubunit interfaces below the agonist binding sites, whereas the M2-M3 linker in one of the α subunits is located at the α/γ intersubunit interface below the BZD binding site (Figs. 1 and S9). Thus, physical location of each M2-M3 linker with respect to either agonist or BZD binding sites in the ECD may explain the subunit-specific effects of α_m, β_m, or γ_m on the intrinsic closed-open equilibrium and its modulation by DZ. In such a case, the M2-M3 linkers of distinct subunits would have asymmetric roles in pore gating and drug modulation, with the β subunit M2-M3 linker having a predominant role in regulating pore opening and the α subunit M2-M3 being most involved in DZ-modulation.

Although grossly symmetric, comparison of structures of α1β2/3γ2 receptors in closed antagonist-bound and desensitized agonist-bound conformations indicates some asymmetry in subunit motions. For example, the ECDs of β subunits rotate a few degrees further than other subunits, the M2-M3 linkers of β subunits undergo the largest radial expansion, and the pore gate 9′ leucine in β subunits rotate furthest out of the ion-conducting pathway (Fig. 8) (20,21). Observations for disulfide bond formation and zinc binding to introduced cysteines also suggest asymmetric flexibility between α and β subunits near the top of the M2 helix (57). From a functional perspective, mutation of a conserved lysine in the M2-M3 linker that is associated with human epilepsy (α1(K278M), β2(K274M), γ2(K289M)) has subunit-specific effects on receptor activity (58,59). Thus, the asymmetric effects of alanine substitutions in distinct M2-M3 linkers on pore gating and DZ modulation that we observe here may reflect distinct conformational changes in specific subunits or at specific intersubunit interfaces. However, our observations only suggest that the subunits contribute to the energetics of these processes differentially. Global conformational changes that are grossly symmetric among all subunits, but for which distinct subunit M2-M3 linkers contribute differentially to the energetics, are entirely compatible with our results.

Here, we show that the central residue in the M2-M3 linkers of β2 versus α1 and γ2 subunits have opposing roles in regulating the intrinsic unliganded closed-open

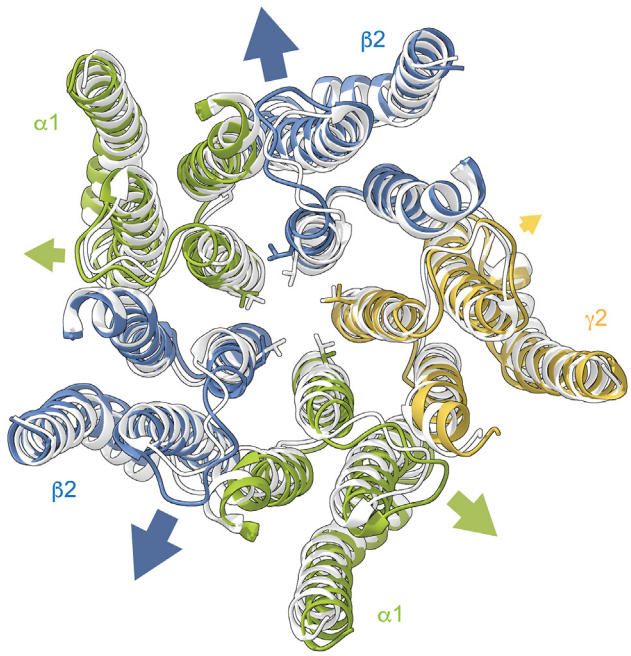

FIGURE 8 Asymmetric M2-M3 linker and M2 helix motions during channel gating. Comparison of the TMD for cryo-EM structures of α1β2γ2 receptors in complex with either the antagonist bicuculline (*light gray*, closed conformation; PDB: 6X3S) or GABA (*colored subunits*, desensitized conformation; PDB: 6X3Z). TMD helices were aligned in ChimeraX (56). The ECD is omitted for clarity. Top-down view looking through the channel into the cell. The 9′ leucines forming the central pore gate are shown as sticks. Comparison of closed versus desensitized conformations indicative of motions occurring during pore opening indicates a relatively larger radial displacement of the M2-M3 linker and rotation of the 9′ leucine out of the conducting pathway in β2 subunits compared with α1 or γ2 subunits (*arrows*).

equilibrium. In contrast, only this position in the α1 subunit regulates the efficiency of modulation of this equilibrium by DZ. These observations shed new light on the subunit-specific roles of M2-M3 linkers which correlate structurally with their respective ligand-binding intersubunit interfaces.

SUPPORTING MATERIAL

Supporting material can be found online at https://doi.org/10.1016/j.bpj.2024.02.016.

AUTHOR CONTRIBUTIONS

J.W.N. carried out the experiments and contributed to writing of the manuscript. Z.E. carried out the experiments, performed the analysis, and generated the data visualizations. M.P.G.-O. conceived, designed, and oversaw the project, and contributed to writing of the manuscript.

ACKNOWLEDGMENTS

We thank Dr. Cynthia Czajkowski for gifting DNA for wild-type $GABA_AR$ subunits, Drs. Richard Aldrich, Eric Senning, Andres Jara-Oseguera, Harold Zakon, and Amy Lee for insightful feedback, and Dr. Richard Aldrich for shared use of equipment.

DECLARATION OF INTERESTS

The authors declare no competing interests.

REFERENCES

1. Smart, T. G., and F. A. Stephenson. 2019. A half century of γ-aminobutyric acid. *Brain Neurosci. Adv.* 3, 2398212819858249. https://doi.org/10.1177/2398212819858249.
2. Pless, S. A., and L. G. Sivilotti. 2019. A tale of ligands big and small: an update on how pentameric ligand-gated ion channels interact with agonists and proteins. *Curr. Opin. Physiol.* 2:19–26. https://doi.org/10.1016/j.cophys.2017.12.012.
3. Braat, S., and R. F. Kooy. 2015. The GABAA receptor as a therapeutic target for neurodevelopmental disorders. *Neuron.* 86:1119–1130. https://doi.org/10.1016/j.neuron.2015.03.042.
4. Gao, F., L. Qi, …, H. Zhao. 2018. Impaired GABA neural circuits are critical for fragile X syndrome. *Neural Plast.* 2018, 8423420. https://doi.org/10.1155/2018/8423420.
5. Ghit, A., D. Assal, …, D. E. E. Hussein. 2021. GABAA receptors: structure, function, pharmacology, and related disorders. *J. Genet. Eng. Biotechnol.* 19:123. https://doi.org/10.1186/s43141-021-00224-0.
6. Hernandez, C. C., and R. L. Macdonald. 2019. A structural look at GABAA receptor mutations linked to epilepsy syndromes. *Brain Res.* 1714:234–247. https://doi.org/10.1016/j.brainres.2019.03.004.
7. Mahdavi, M., M. Kheirollahi, …, M. Mirsafaie. 2018. Meta-Analysis of the Association between GABA Receptor Polymorphisms and Autism Spectrum Disorder (ASD). *J. Mol. Neurosci.* 65:1–9. https://doi.org/10.1007/s12031-018-1073-7.
8. Ramamoorthi, K., and Y. Lin. 2011. The contribution of GABAergic dysfunction to neurodevelopmental disorders. *Trends Mol. Med.* 17:452–462. https://doi.org/10.1016/j.molmed.2011.03.003.
9. Solís-Añez, E., W. Delgado-Luengo, and M. L. Hernández. 2007. [Autism, chromosome 15 and the GAbaergic dysfunction hypothesis]. *Invest. Clin.* 48:529–541.
10. Agarwal, S. D., and B. E. Landon. 2019. Patterns in outpatient benzodiazepine prescribing in the United States. *JAMA Netw. Open.* 2, e187399. https://doi.org/10.1001/jamanetworkopen.2018.7399.
11. Möhler, H., J. M. Fritschy, and U. Rudolph. 2002. A new benzodiazepine pharmacology. *J. Pharmacol. Exp. Therapeut.* 300:2–8. https://doi.org/10.1124/jpet.300.1.2.
12. Goldschen-Ohm, M. P. 2022. Benzodiazepine modulation of GABAA receptors: A mechanistic perspective. *Biomolecules.* 12, 1784. https://doi.org/10.3390/biom12121784.
13. Olsen, R. W., and W. Sieghart. 2008. International Union of Pharmacology. LXX. Subtypes of gamma-aminobutyric acid(A) receptors: classification on the basis of subunit composition, pharmacology, and function. Update. *Pharmacol. Rev.* 60:243–260. https://doi.org/10.1124/pr.108.00505.
14. Sieghart, W., and G. Sperk. 2002. Subunit composition, distribution and function of GABA(A) receptor subtypes. *Curr. Top. Med. Chem.* 2:795–816. https://doi.org/10.2174/1568026023393507.
15. Jha, A., D. J. Cadugan, …, A. Auerbach. 2007. Acetylcholine receptor gating at extracellular transmembrane domain interface: the cys-loop and M2-M3 linker. *J. Gen. Physiol.* 130:547–558. https://doi.org/10.1085/jgp.200709856.
16. Kaczor, P. T., M. A. Michałowski, and J. W. Mozrzymas. 2022. α1 Proline 277 Residues Regulate GABAAR Gating through M2-M3 Loop Interaction in the Interface Region. *ACS Chem. Neurosci.* 13:3044–3056. https://doi.org/10.1021/acschemneuro.2c00401.
17. Kash, T. L., A. Jenkins, …, N. L. Harrison. 2003. Coupling of agonist binding to channel gating in the GABA(A) receptor. *Nature.* 421:272–275. https://doi.org/10.1038/nature01280.
18. O'Shea, S. M., and N. L. Harrison. 2000. Arg-274 and Leu-277 of the gamma-aminobutyric acid type A receptor alpha 2 subunit define agonist efficacy and potency. *J. Biol. Chem.* 275:22764–22768. https://doi.org/10.1074/jbc.M001299200.
19. Sigel, E., A. Buhr, and R. Baur. 1999. Role of the conserved lysine residue in the middle of the predicted extracellular loop between M2 and M3 in the GABA(A) receptor. *J. Neurochem.* 73:1758–1764. https://doi.org/10.1046/j.1471-4159.1999.731758.x.
20. Kim, J. J., A. Gharpure, …, R. E. Hibbs. 2020. Shared structural mechanisms of general anaesthetics and benzodiazepines. *Nature.* 585:303–308. https://doi.org/10.1038/s41586-020-2654-5.
21. Masiulis, S., R. Desai, …, A. R. Aricescu. 2019. GABAA receptor signalling mechanisms revealed by structural pharmacology. *Nature.* 565:454–459. https://doi.org/10.1038/s41586-018-0832-5.
22. Nemecz, Á., M. S. Prevost, …, P.-J. Corringer. 2016. Emerging Molecular Mechanisms of Signal Transduction in Pentameric Ligand-Gated Ion Channels. *Neuron.* 90:452–470. https://doi.org/10.1016/j.neuron.2016.03.032.
23. Nors, J. W., S. Gupta, and M. P. Goldschen-Ohm. 2021. A critical residue in the α1M2-M3 linker regulating mammalian GABAA receptor pore gating by diazepam. *Elife.* 10, e64400. https://doi.org/10.7554/eLife.64400.
24. Baur, R., and E. Sigel. 2005. Benzodiazepines affect channel opening of GABA A receptors induced by either agonist binding site. *Mol. Pharmacol.* 67:1005–1008. https://doi.org/10.1124/mol.104.008151.
25. Goldschen-Ohm, M. P., D. A. Wagner, …, M. V. Jones. 2010. An epilepsy-related region in the GABA(A) receptor mediates long-distance effects on GABA and benzodiazepine binding sites. *Mol. Pharmacol.* 77:35–45. https://doi.org/10.1124/mol.109.058289.
26. Sancar, F., and C. Czajkowski. 2011. Allosteric modulators induce distinct movements at the GABA-binding site interface of the GABA-A receptor. *Neuropharmacology.* 60:520–528. https://doi.org/10.1016/j.neuropharm.2010.11.009.
27. Sharkey, L. M., and C. Czajkowski. 2008. Individually monitoring ligand-induced changes in the structure of the GABAA receptor at benzodiazepine binding site and non-binding-site interfaces. *Mol. Pharmacol.* 74:203–212. https://doi.org/10.1124/mol.108.044891.
28. Venkatachalan, S. P., and C. Czajkowski. 2012. Structural link between γ-aminobutyric acid type A (GABAA) receptor agonist binding site

and inner β-sheet governs channel activation and allosteric drug modulation. *J. Biol. Chem.* 287:6714–6724. https://doi.org/10.1074/jbc.M111.316836.

29. Williams, D. B., and M. H. Akabas. 2000. Benzodiazepines induce a conformational change in the region of the gamma-aminobutyric acid type A receptor alpha(1)-subunit M3 membrane-spanning segment. *Mol. Pharmacol.* 58:1129–1136. https://doi.org/10.1124/mol.58.5.1129.
30. Zhu, S., A. Sridhar, …, R. E. Hibbs. 2022. Structural and dynamic mechanisms of GABAA receptor modulators with opposing activities. *Nat. Commun.* 13:4582. https://doi.org/10.1038/s41467-022-32212-4.
31. Walters, R. J., S. H. Hadley, …, J. Amin. 2000. Benzodiazepines act on GABAA receptors via two distinct and separable mechanisms. *Nat. Neurosci.* 3:1274–1281. https://doi.org/10.1038/81800.
32. Chang, Y., and D. S. Weiss. 1999. Allosteric activation mechanism of the alpha 1 beta 2 gamma 2 gamma-aminobutyric acid type A receptor revealed by mutation of the conserved M2 leucine. *Biophys. J.* 77:2542–2551. https://doi.org/10.1016/s0006-3495(99)77089-x.
33. Rüsch, D., and S. A. Forman. 2005. Classic benzodiazepines modulate the open-close equilibrium in alpha1beta2gamma2L gamma-aminobutyric acid type A receptors. *Anesthesiology.* 102:783–792. https://doi.org/10.1097/00000542-200504000-00014.
34. Scheller, M., and S. A. Forman. 2002. Coupled and uncoupled gating and desensitization effects by pore domain mutations in GABA(A) receptors. *J. Neurosci.* 22:8411–8421.
35. Bianchi, M. T., and R. L. Macdonald. 2001. Mutation of the 9' leucine in the GABA(A) receptor gamma2L subunit produces an apparent decrease in desensitization by stabilizing open states without altering desensitized states. *Neuropharmacology.* 41:737–744. https://doi.org/10.1016/s0028-3908(01)00132-0.
36. Purohit, P., and A. Auerbach. 2009. Unliganded gating of acetylcholine receptor channels. *Proc. Natl. Acad. Sci. USA.* 106:115–120. https://doi.org/10.1073/pnas.0809272106.
37. Colquhoun, D. 1998. Binding, gating, affinity and efficacy: the interpretation of structure-activity relationships for agonists and of the effects of mutating receptors. *Br. J. Pharmacol.* 125:924–947. https://doi.org/10.1038/sj.bjp.0702164.
38. Boileau, A. J., R. Baur, …, C. Czajkowski. 2002. The relative amount of cRNA coding for gamma2 subunits affects stimulation by benzodiazepines in GABA(A) receptors expressed in Xenopus oocytes. *Neuropharmacology.* 43:695–700. https://doi.org/10.1016/s0028-3908(02)00036-9.
39. Holt, J. M., and G. K. Ackers. 2009. Chapter 7 the hill coefficient. *In* Biothermodynamics, Part A Elsevier, pp. 193–212. https://doi.org/10.1016/S0076-6879(08)04207-9.
40. Prinz, H. 2010. Hill coefficients, dose-response curves and allosteric mechanisms. *J. Chem. Biol.* 3:37–44. https://doi.org/10.1007/s12154-009-0029-3.
41. Sente, A., R. Desai, …, A. R. Aricescu. 2022. Differential assembly diversifies GABAA receptor structures and signalling. *Nature.* 604:190–194. https://doi.org/10.1038/s41586-022-04517-3.
42. Goldschen-Ohm, M. P., A. Haroldson, …, R. A. Pearce. 2014. A nonequilibrium binary elements-based kinetic model for benzodiazepine regulation of GABAA receptors. *J. Gen. Physiol.* 144:27–39. https://doi.org/10.1085/jgp.201411183.
43. Campo-Soria, C., Y. Chang, and D. S. Weiss. 2006. Mechanism of action of benzodiazepines on GABAA receptors. *Br. J. Pharmacol.* 148:984–990. https://doi.org/10.1038/sj.bjp.0706796.
44. Li, P., M. M. Eaton, …, G. Akk. 2013. The benzodiazepine diazepam potentiates responses of α1β2γ2L γ-aminobutyric acid type A receptors activated by either γ-aminobutyric acid or allosteric agonists. *Anesthesiology.* 118:1417–1425. https://doi.org/10.1097/ALN.0b013e318289bcd3.
45. Keramidas, A., and N. L. Harrison. 2010. The activation mechanism of alpha1beta2gamma2S and alpha3beta3gamma2S GABAA receptors. *J. Gen. Physiol.* 135:59–75. https://doi.org/10.1085/jgp.200910317.
46. Mortensen, M., K. A. Wafford, …, B. Ebert. 2003. Pharmacology of GABA(A) receptors exhibiting different levels of spontaneous activity. *Eur. J. Pharmacol.* 476:17–24. https://doi.org/10.1016/s0014-2999(03)02125-3.
47. Gibbs, E., E. Klemm, …, S. Chakrapani. 2023. Conformational transitions and allosteric modulation in a heteromeric glycine receptor. *Nat. Commun.* 14:1363. https://doi.org/10.1038/s41467-023-37106-7.
48. Pierce, S. R., S. Q. Xu, G. Akk…, 2024. Potentiation of the GABAAR reveals variable energetic contributions by etiocholanolone and propofol. *Biophys. J.* 123. https://doi.org/10.1016/j.bpj.2023.09.014.
49. Lavoie, A. M., and R. E. Twyman. 1996. Direct evidence for diazepam modulation of GABAA receptor microscopic affinity. *Neuropharmacology.* 35:1383–1392. https://doi.org/10.1016/s0028-3908(96)00077-9.
50. Perrais, D., and N. Ropert. 1999. Effect of zolpidem on miniature IPSCs and occupancy of postsynaptic GABAA receptors in central synapses. *J. Neurosci.* 19:578–588.
51. Rogers, C. J., R. E. Twyman, and R. L. Macdonald. 1994. Benzodiazepine and beta-carboline regulation of single GABAA receptor channels of mouse spinal neurones in culture. *J. Physiol.* 475:69–82. https://doi.org/10.1113/jphysiol.1994.sp020050.
52. Twyman, R. E., C. J. Rogers, and R. L. Macdonald. 1989. Differential regulation of gamma-aminobutyric acid receptor channels by diazepam and phenobarbital. *Ann. Neurol.* 25:213–220. https://doi.org/10.1002/ana.410250302.
53. Vicini, S., J. M. Mienville, and E. Costa. 1987. Actions of benzodiazepine and beta-carboline derivatives on gamma-aminobutyric acid-activated Cl- channels recorded from membrane patches of neonatal rat cortical neurons in culture. *J. Pharmacol. Exp. Therapeut.* 243:1195–1201.
54. Sun, C., H. Zhu, …, E. Gouaux. 2023. Cryo-EM structures reveal native GABAA receptor assemblies and pharmacology. *Nature.* 622:195–201. https://doi.org/10.1038/s41586-023-06556-w.
55. Du, J., W. Lü, …, E. Gouaux. 2015. Glycine receptor mechanism elucidated by electron cryo-microscopy. *Nature.* 526:224–229. https://doi.org/10.1038/nature14853.
56. Pettersen, E. F., T. D. Goddard, …, T. E. Ferrin. 2021. UCSF ChimeraX: structure visualization for researchers, educators, and developers. *Protein Sci.* 30:70–82. https://doi.org/10.1002/pro.3943.
57. Horenstein, J., P. Riegelhaupt, and M. H. Akabas. 2005. Differential protein mobility of the gamma-aminobutyric acid, type A, receptor alpha and beta subunit channel-lining segments. *J. Biol. Chem.* 280:1573–1581. https://doi.org/10.1074/jbc.M410881200.
58. Baulac, S., G. Huberfeld, …, E. LeGuern. 2001. First genetic evidence of GABA(A) receptor dysfunction in epilepsy: a mutation in the gamma2-subunit gene. *Nat. Genet.* 28:46–48. https://doi.org/10.1038/ng0501-46.
59. Hales, T. G., T. Z. Deeb, …, C. N. Connolly. 2006. An asymmetric contribution to gamma-aminobutyric type A receptor function of a conserved lysine within TM2-3 of alpha1, beta2, and gamma2 subunits. *J. Biol. Chem.* 281:17034–17043. https://doi.org/10.1074/jbc.M603599200.

Biophysical Journal, Volume *123*

Supplemental information

$GABA_A$ receptor subunit M2-M3 linkers have asymmetric roles in pore gating and diazepam modulation

Joseph W. Nors, Zachary Endres, and Marcel P. Goldschen-Ohm

Supplemental Material for: $GABA_A$ receptor subunit M2-M3 linkers have asymmetric roles in pore gating and diazepam modulation

Joseph W. Nors[1,2,†], Zachary Endres[1,†], and Marcel P. Goldschen-Ohm[1,*]

[1]Department of Neuroscience, University of Texas at Austin, Austin, TX, USA
[2]Department of Molecular and Cellular Physiology, Stanford University, Stanford, CA, USA
[†]Co-first author
*Corresponding author

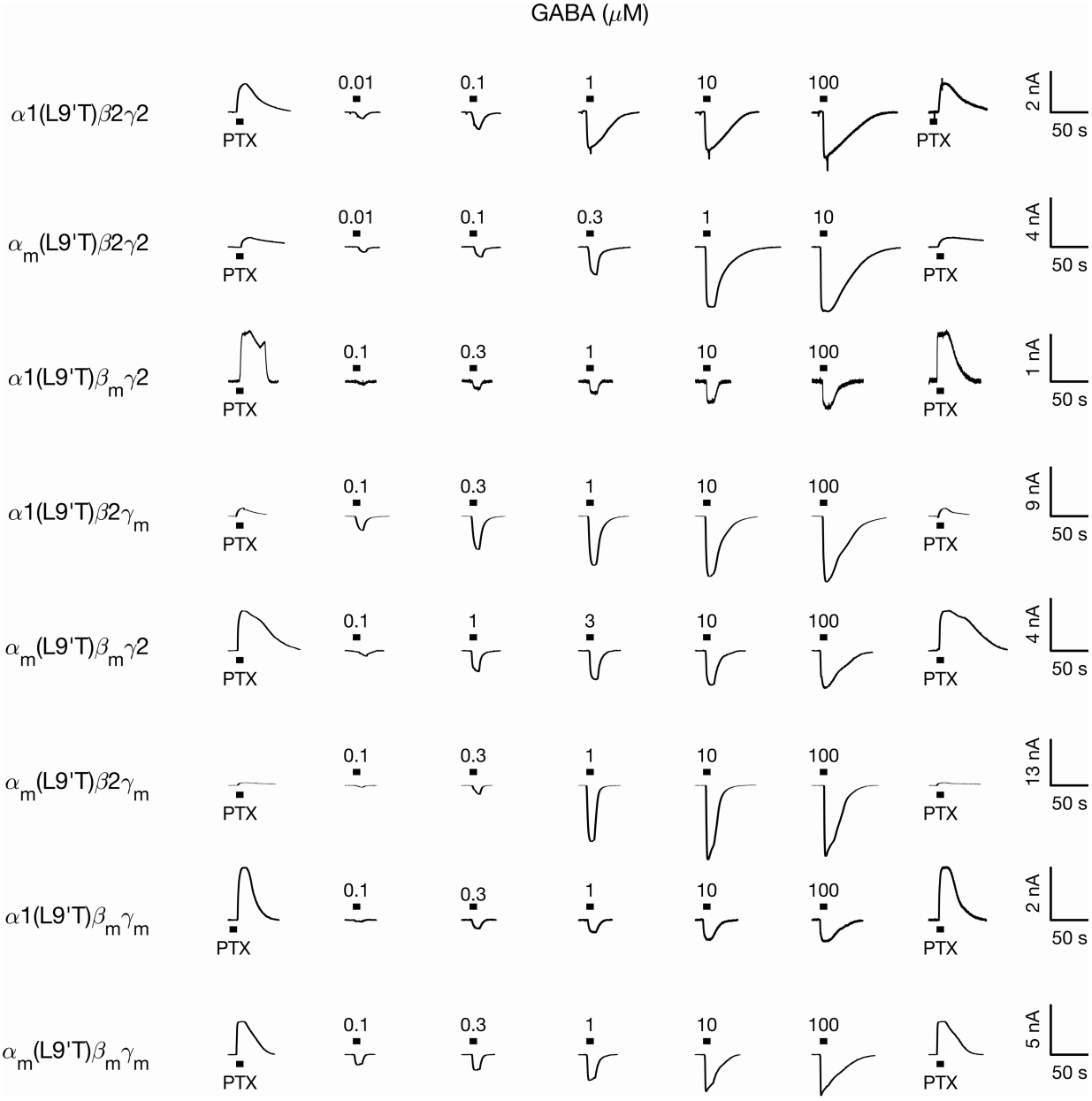

Figure S1. Example GABA-evoked currents from receptors with M2-M3 linker mutations α_m, β_m, and/or γ_m in the gain-of-function α1(L9'T)β2γ2 background. Currents are in response to 10 second pulses (black bars) of either 1 mM PTX or a series of increasing concentrations of GABA (concentration in micromolar above respective black bar). Summaries of concentration-response curves across oocytes are shown in **Figure S4**. Responses to GABA were bookended by the pore blocker PTX to assess the amount of spontaneous unliganded activity and identify the zero-current baseline.

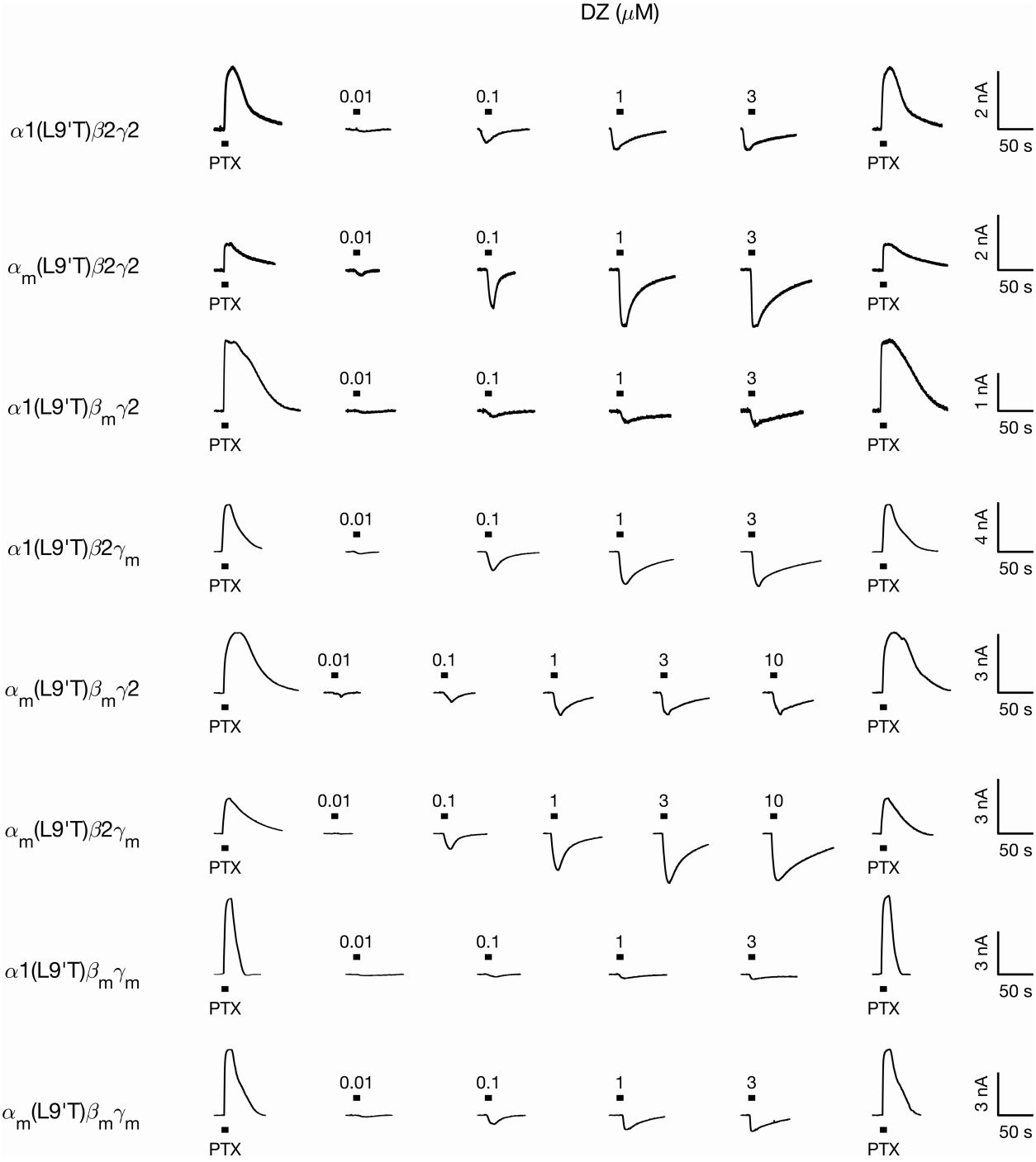

Figure S2. Example DZ-evoked currents from receptors with M2-M3 linker mutations α_m, β_m, and/or γ_m in the gain-of-function α1(L9'T)β2γ2 background. Currents are in response to 10 second pulses (black bars) of either 1 mM PTX or a series of increasing concentrations of DZ (concentration in micromolar above respective black bar). Summaries of concentration-response curves across oocytes are shown in **Figure S5**. Responses to DZ were bookended by the pore blocker PTX to assess the amount of spontaneous unliganded activity and identify the zero-current baseline.

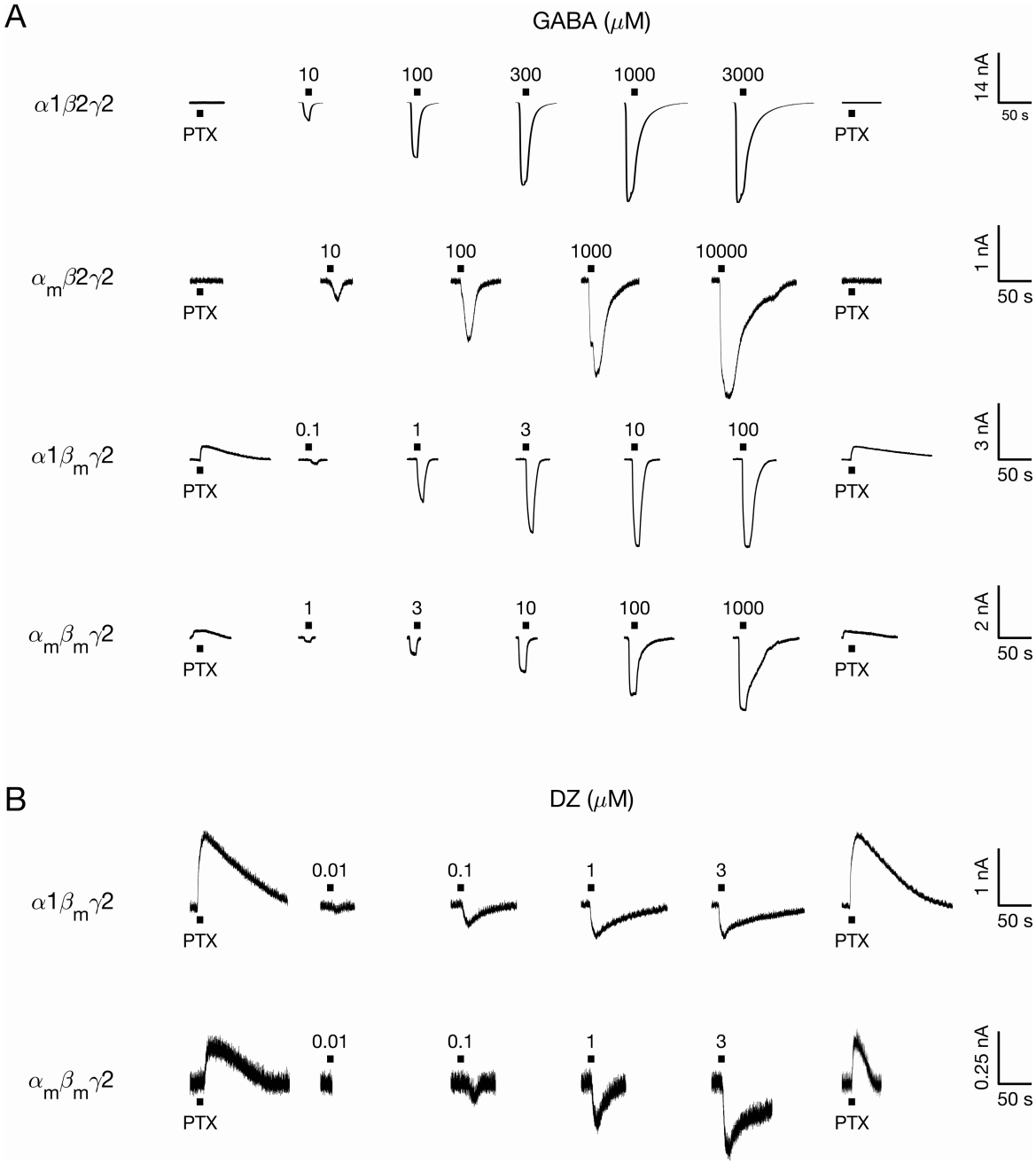

Figure S3. Example GABA- or DZ-evoked currents from receptors with M2-M3 linker mutations α_m, β_m, and/or γ_m in a wild type $\alpha1\beta2\gamma2$ background. (A) Currents are in response to 10 second pulses (black bars) of either 1 mM PTX or a series of increasing concentrations of GABA (concentration in micromolar above respective black bar). Summaries of concentration-response curves across oocytes are shown in **Figure S6**. Responses to GABA were bookended by the pore blocker PTX to assess the amount of spontaneous unliganded activity and identify the zero-current baseline. **(B)** Same as in **(A)** except for currents evoked with DZ instead of GABA.

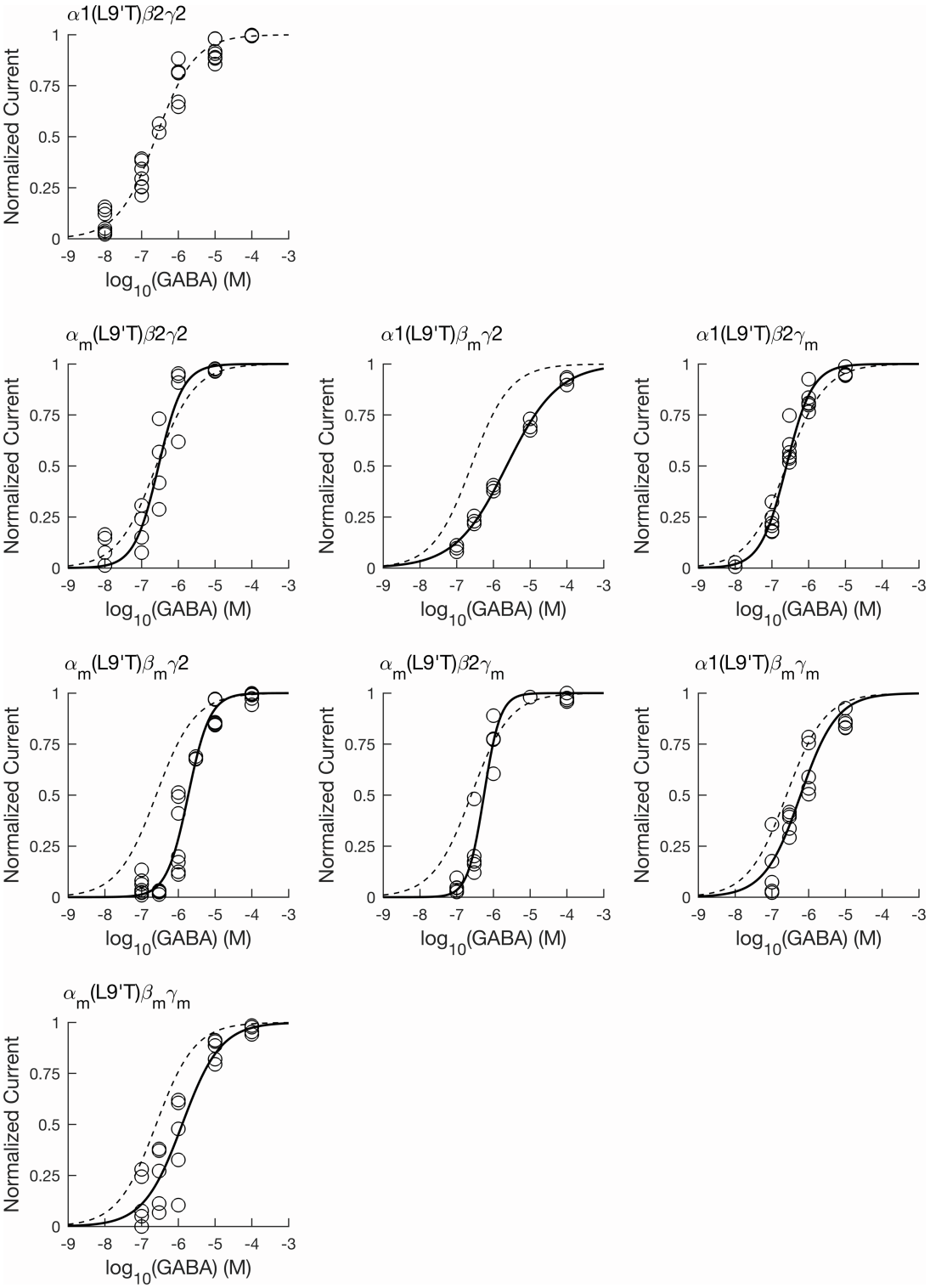

Figure S4. GABA-evoked concentration-response relationships for gain-of-function α1(L9'T)β2γ2 receptors without and with M2-M3 linker mutations α_m, β_m, and/or γ_m. For each oocyte, GABA-evoked current amplitudes from the unliganded baseline as shown in **Figure S1** versus GABA concentration were fit to the Hill equation **(Equation 1)**. Parameters for individual fits are shown in **Figure S7**. Data points for each oocyte where normalized to their Hill fit maximum, and the

combined normalized data from all oocytes (circles) was fit to the Hill equation with $I_{max} = 1$ (solid lines, dashed line is fit for α1(L9'T)β2γ2 receptors). Combined fit parameters (EC_{50}, Hill coefficient *h*) and number of oocytes (n) for each construct: α1(L9'T)β2γ2: EC_{50} = 0.25 μM, *h* = 0.83, n = 7, α_m(L9'T)β2γ2: EC_{50} = 0.29 μM, *h* = 1.31, n = 4, α1(L9'T)$\beta_m\gamma$2: EC_{50} = 2.28 μM, *h* = 0.62, n = 3, α1(L9'T)β2γ_m: EC_{50} = 0.25 μM, *h* = 1.23, n = 6, α_m(L9'T)$\beta_m\gamma$2: EC_{50} = 1.86 μM, *h* = 1.47, n = 7, α_m(L9'T)β2γ_m: EC_{50} = 0.53 μM, *h* = 1.95, n = 5, α1(L9'T)$\beta_m\gamma_m$: EC_{50} = 0.6 μM, *h* = 0.88, n = 5, α_m(L9'T)$\beta_m\gamma_m$: EC_{50} = 1.27 μM, *h* = 0.83 , n = 5.

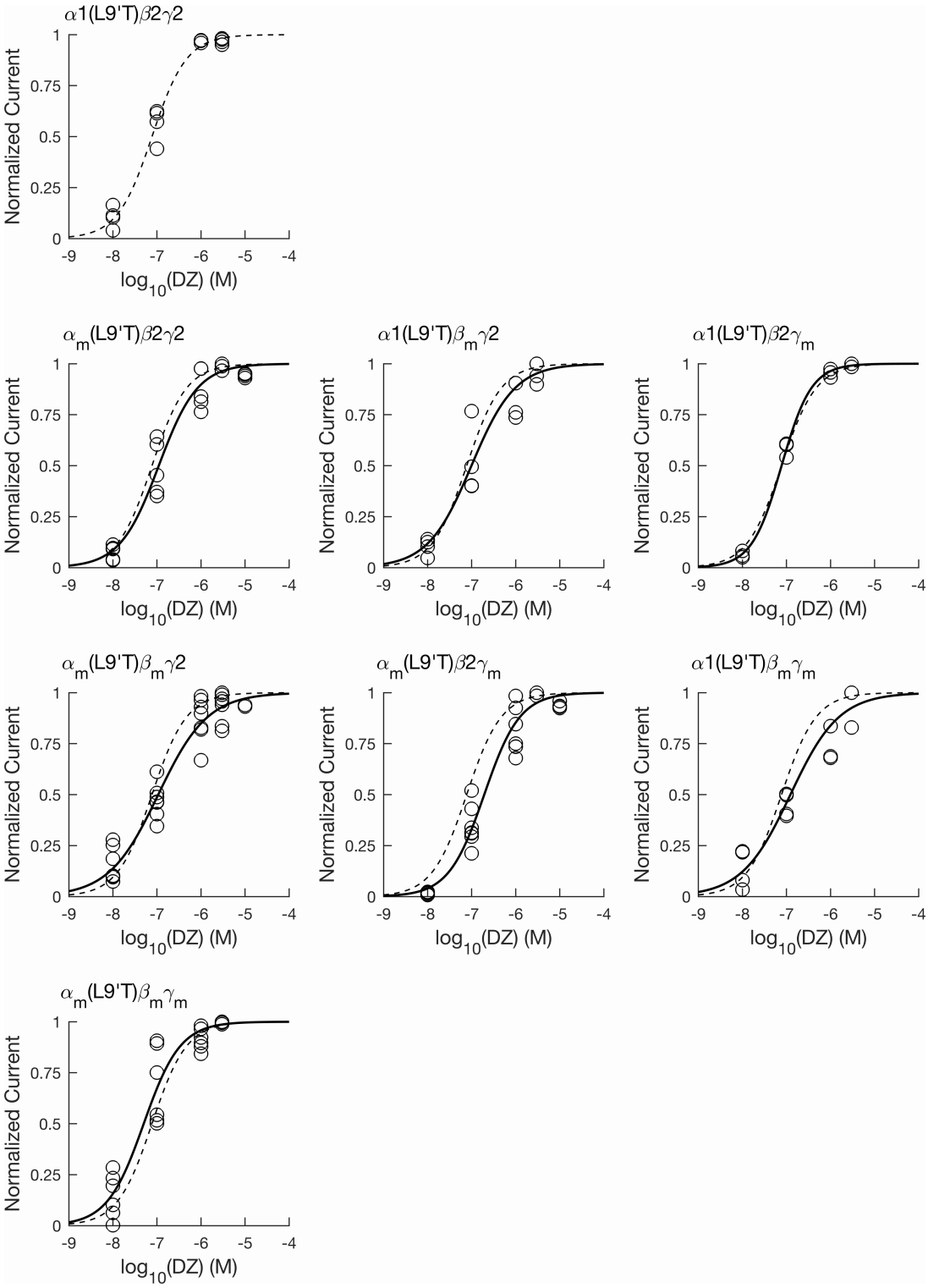

Figure S5. DZ-evoked concentration-response relationships for gain-of-function α1(L9'T)β2γ2 receptors without and with M2-M3 linker mutations α_m, β_m, and/or γ_m. For each oocyte, DZ-evoked current amplitudes from the unliganded baseline as shown in **Figure S2** versus DZ concentration were fit to the Hill equation **(Equation 1)**. Parameters for individual fits are shown in **Figure S8**. Data points for each oocyte where normalized to their Hill fit maximum, and the combined

normalized data from all oocytes (circles) was fit to the Hill equation with $I_{max} = 1$ (solid lines, dashed line is fit for α1(L9'T)β2γ2 receptors). Combined fit parameters (EC_{50}, Hill coefficient *h*) and number of oocytes (n) for each construct: α1(L9'T)β2γ2: EC_{50} = 0.08 μM, *h* = 1.10, n = 4, α_m(L9'T)β2γ2: EC_{50} = 0.11 μM, *h* = 0.98, n = 5, α1(L9'T)$\beta_m\gamma$2: EC_{50} = 0.1 μM, *h* = 0.88, n = 4, α1(L9'T)β2γ_m: EC_{50} = 0.08 μM, *h* = 1.28, n = 3, α_m(L9'T)$\beta_m\gamma$2: EC_{50} = 0.11 μM, *h* = 0.77, n = 7, α_m(L9'T)β2γ_m: EC_{50} = 0.19 μM, *h* = 1.07, n = 7, α1(L9'T)$\beta_m\gamma_m$: EC_{50} = 0.12 μM, *h* = 0.79, n = 4, α_m(L9'T)$\beta_m\gamma_m$: EC_{50} = 0.05 μM, *h* = 1.05, n = 6.

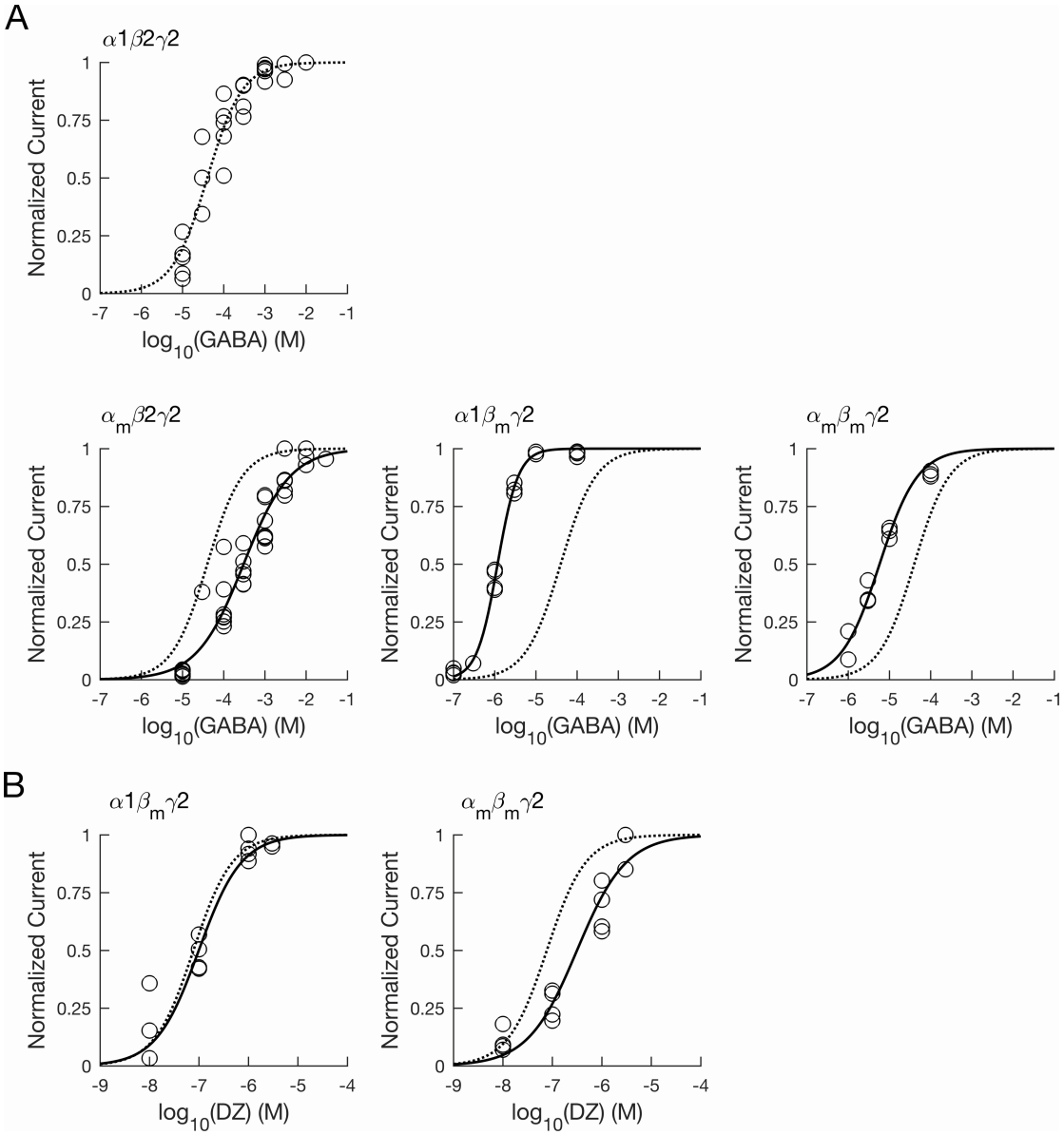

Figure S6. GABA- and DZ-evoked concentration-response relationships for wild type α1β2γ2 receptors without and with M2-M3 linker mutations α_m, β_m, and/or γ_m. For each oocyte, GABA- **(A)** or DZ-evoked **(B)** current amplitudes from the unliganded baseline as shown in **Figure S3** versus GABA or DZ concentration, respectively, were fit to the Hill equation **(Equation 1)**. Parameters for individual fits are shown in **Figures S7-S8**. Data points for each oocyte where normalized to their Hill fit maximum, and the combined normalized data from all oocytes (circles) was fit to the Hill equation with $I_{max} = 1$ (solid lines, dashed line is fit for α1β2γ2 receptors). GABA-evoked **(A)** combined fit parameters (EC_{50}, Hill coefficient *h*) and number of oocytes (n) for each construct: α1β2γ2: EC_{50} = 39.94 μM, *h* = 1.02, n = 5, α_mβ2γ2: EC_{50} = 303.37 μM, *h* = 0.77, n = 7, α1β_mγ2: EC_{50} = 1.17 μM, *h* = 1.73, n = 4, $\alpha_m\beta_m$γ2: EC_{50} = 5.76 μM, *h* = 0.94, n = 3. DZ-evoked **(B)** combined fit parameters (EC_{50}, Hill coefficient *h*) and number of oocytes (n) for each construct: α1β_mγ2: EC_{50} = 0.1 μM, *h* = 1.01, n = 4, $\alpha_m\beta_m$γ2: EC_{50} = 0.31 μM, *h* = 0.87, n = 4.

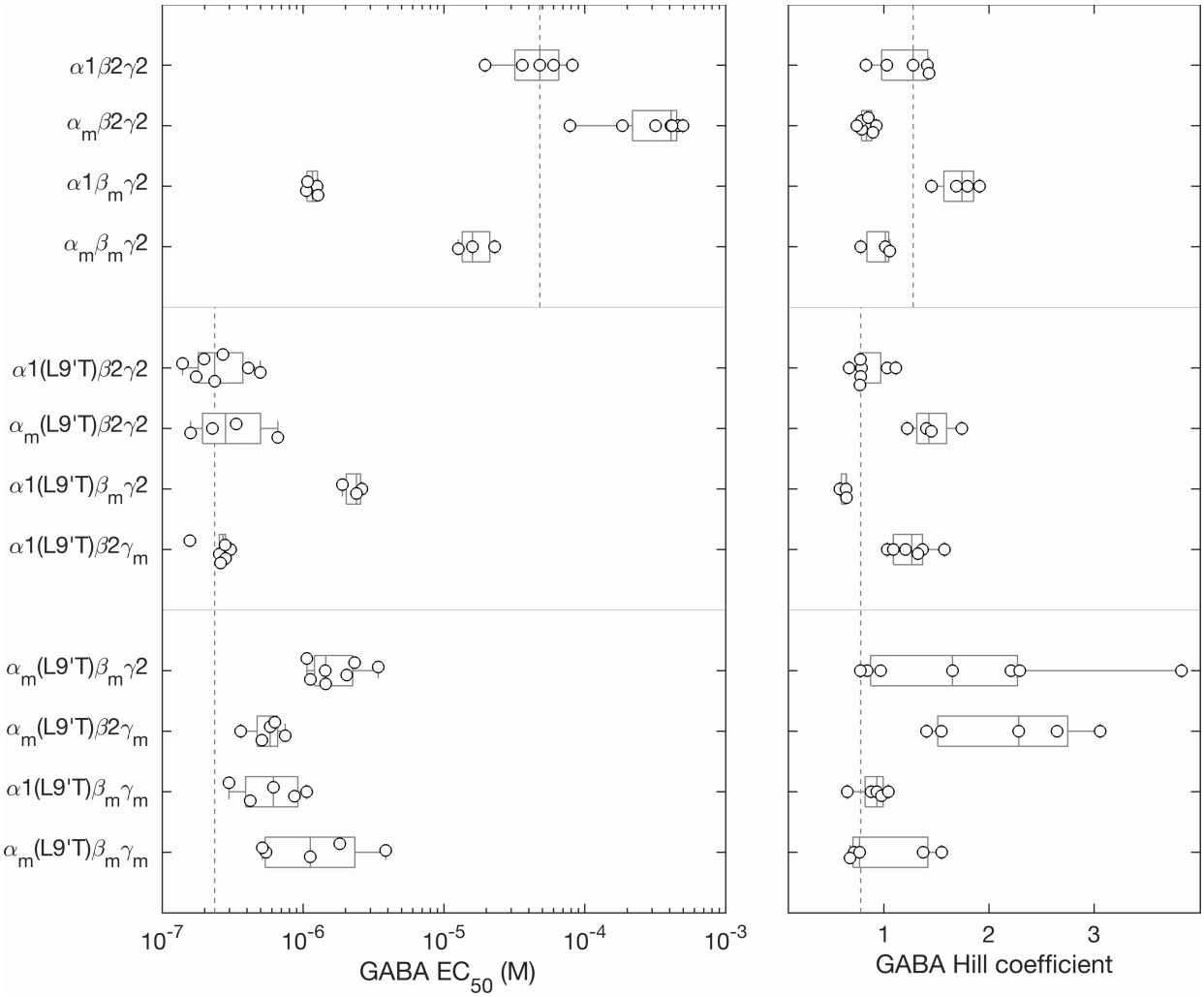

Figure S7. Summary of GABA concentration-response relation Hill fit parameters for individual oocytes. Data points are for individual oocytes ($\alpha1\beta2\gamma2$: n = 5; $\alpha_m\beta2\gamma2$: n = 7; $\alpha1\beta_m\gamma2$: n = 4; $\alpha_m\beta_m\gamma2$: n = 3; $\alpha1$(L9'T)$\beta2\gamma2$: n = 7; α_m(L9'T)$\beta2\gamma2$: n = 4 ; $\alpha1$(L9'T)$\beta_m\gamma2$: n = 3; $\alpha1$(L9'T)$\beta2\gamma_m$: n = 6; α_m(L9'T)$\beta_m\gamma2$: n = 7 ; α_m(L9'T)$\beta2\gamma_m$: n = 5 ; $\alpha1$(L9'T)$\beta_m\gamma_m$: n = 5 ; α_m(L9'T)$\beta_m\gamma_m$: n = 5). Box plots indicate quartiles, and the upper and lower vertical dashed lines are the median for the $\alpha1$(L9'T)$\beta2\gamma2$ and $\alpha1\beta2\gamma2$ backgrounds, respectively.

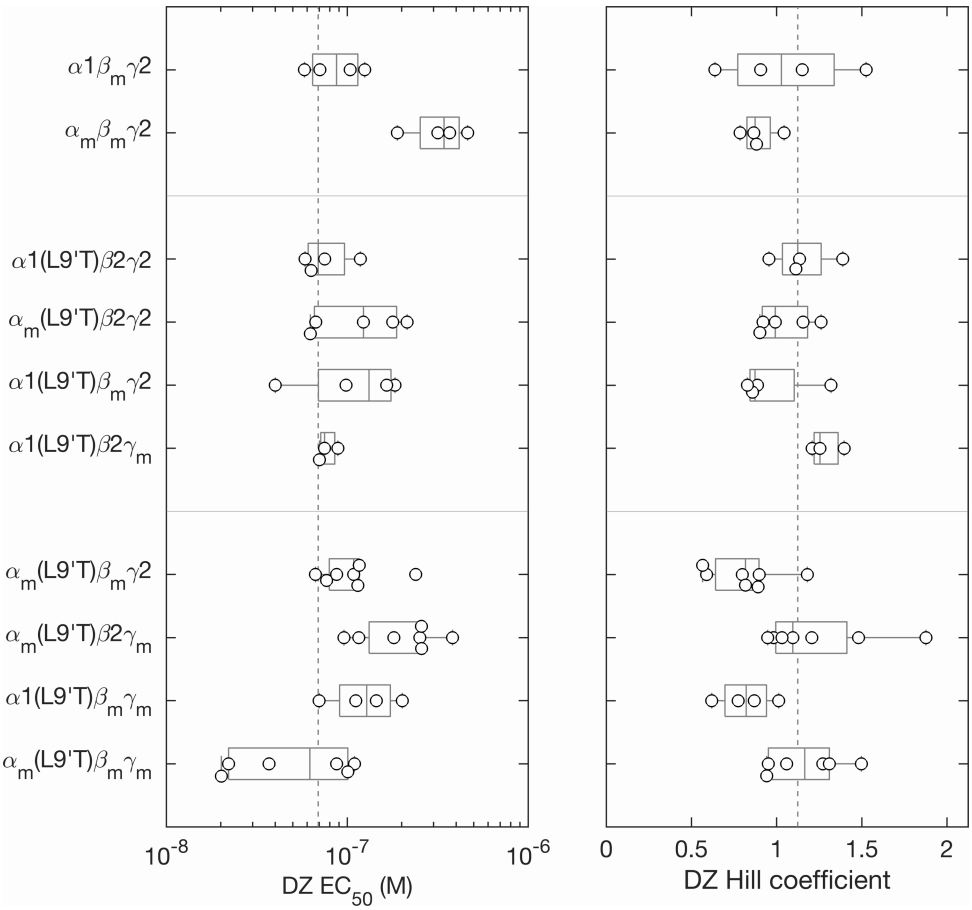

Figure S8. Summary of DZ concentration-response relation Hill fit parameters for individual oocytes. Data points are for individual oocytes ($\alpha1\beta_m\gamma2$: n = 4; $\alpha_m\beta_m\gamma2$: n = 4; $\alpha1$(L9'T)$\beta2\gamma2$: n = 4; α_m(L9'T)$\beta2\gamma2$: n = 5; $\alpha1$(L9'T)$\beta_m\gamma2$: n = 4; $\alpha1$(L9'T)$\beta2\gamma_m$: n = 3; α_m(L9'T)$\beta_m\gamma2$: n = 7; α_m(L9'T)$\beta2\gamma_m$: n = 7; $\alpha1$(L9'T)$\beta_m\gamma_m$: n = 4; α_m(L9'T)$\beta_m\gamma_m$: n = 6). Box plots indicate quartiles, and the vertical dashed line is the median for the $\alpha1$(L9'T)$\beta2\gamma2$ background.

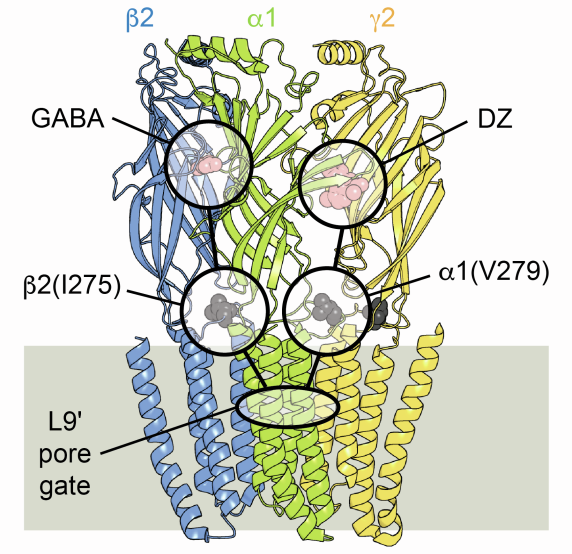

Figure S9. Functional asymmetry in M2-M3 linkers may correspond to the ligand binding interface in which the linker is located. Side-on view from the plane of the membrane omitting back two subunits for clarity. Subunits α1, β2, and γ2 are shown in green, blue, and yellow, respectively. The relative locations of bound GABA or DZ and M2-M3 linker residues β2(I275) or α1(V279) at β/α or α/γ intersubunit interfaces, respectively, and the 9' leucine pore gate are highlighted.